

Perturbative renormalization of the Ginzburg–Landau model revisited

J. Kaupužs *

Institute of Mathematics and Computer Science, University of Latvia
29 Raiņa Boulevard, LV–1459 Riga, Latvia

May 4, 2021

Abstract

The perturbative renormalization of the Ginzburg–Landau model is reconsidered based on the Feynman diagram technique. We derive renormalization group (RG) flow equations, exactly calculating all vertices appearing in the perturbative renormalization of the φ^4 model up to the ε^3 order of the ε -expansion. In this case, the φ^2 , φ^4 , φ^6 , and φ^8 vertices appear. All these vertices are relevant. We have tested the expected basic properties of the RG flow, such as the semigroup property. Under repeated RG transformation R_s , appropriately represented RG flow on the critical surface converges to certain s -independent fixed point. The Fourier-transformed two-point correlation function $G(\mathbf{k})$ has been considered. Although the ε -expansion of $X(\mathbf{k}) = 1/G(\mathbf{k})$ is well defined on the critical surface, we have revealed an inconsistency of the perturbative method with the exact rescaling of $X(\mathbf{k})$, represented as an expansion in powers of k at $k \rightarrow 0$. We have discussed also some aspects of the perturbative renormalization of the two-point correlation function slightly above the critical point. Apart from the ε -expansion, we have tested and briefly discussed also a modified approach, where the φ^4 coupling constant u is the expansion parameter at a fixed spatial dimensionality d .

Keywords: renormalization group, ε -expansion, critical phenomena

1 Introduction

The perturbative renormalization of the Ginzburg–Landau (or φ^4) model has a long history (see [1, 2, 3, 4] and references therein). However, as mentioned in [2], a complete formulation of the renormalization group (RG) beyond the ε^2 order of the ε -expansion (where $\varepsilon = 4 - d > 0$, d being the spatial dimensionality) met mathematical difficulties, which could not be overcome. In fact, the ε -expansion of the critical exponents beyond the lowest orders is based on an alternative approach, which relies on the Callan-Symanzik equation [5, 6, 7]. The latter one represents a scaling property of the φ^4 model [5], and the method is based on a set of assumptions [7]. Since the perturbative RG theory is not rigorous, stringent tests of its validity and consistency make sense. Our aim is to perform such tests.

We have tested the expected basic properties of the RG flow. Following the idea in [8], we have checked the semigroup property $R_{s_1 s_2} \mu = R_{s_2} R_{s_1} \mu$, where R_s is the RG operator with

*E-mail: kaupuzs@latnet.lv

scale factor $s > 1$ acting on the set of Hamiltonian parameters μ . We have tested the expected s -independence of the fixed point μ^* , as well as the scaling of the Fourier-transformed two-point correlation function $G(\mathbf{k})$ on the critical surface.

Another strategy of verification has been used in [9], considering a four-dimensional ($d = 4$) model with Gaussian measure modified in such a way to simulate $d = 4 - \varepsilon$ dimensions with ε small and positive. This method allows to control rigorously the remainder of the perturbation series. The obtained results [9] confirm the existence of the non-Gaussian fixed point at a distance $\mathcal{O}(\varepsilon)$ away from the Gaussian one as proposed earlier [1] by the ε -expansion. However, the expected decay of the two-point correlation function appears to be canonical (i. e., Gaussian, see Introduction part in [9]) in disagreement with that provided by the ε -expansion and observed in ordinary spin systems of dimensionality $d < 4$ like, e. g., three-dimensional and two-dimensional Ising models. In view of these observations, the classical (used in the ε -expansion) way of introduction of non-integer spatial dimensionality d via an analytic continuation from d -dimensional hypercubes appears to be more meaningful than that in [9]. In fact, there is no unique definition of the non-integer d . It can be introduced in a more physical way as a suitable “fractal” dimension of an irregular lattice [10, 11].

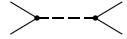

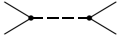
2 Diagrammatic formulation of the renormalization

As a starting point, we consider a φ^4 model with the Hamiltonian H defined by

$$H/T = \int \frac{r}{2} \varphi^2(\mathbf{x}) + \frac{c}{2} (\nabla \varphi(\mathbf{x}))^2 + \frac{1}{8} \int \int \varphi^2(\mathbf{x}_1) u(\mathbf{x}_1 - \mathbf{x}_2) \varphi^2(\mathbf{x}_2) d\mathbf{x}_1 d\mathbf{x}_2, \quad (1)$$

where the order parameter $\varphi(\mathbf{x})$ is an n -component vector with components $\varphi_i(\mathbf{x})$, depending on the coordinate \mathbf{x} , and T is the temperature. The field $\varphi_j(\mathbf{x})$ is given in Fourier representation by $\varphi_j(\mathbf{x}) = V^{-1/2} \sum_{k < \Lambda} \varphi_{j,\mathbf{k}} e^{i\mathbf{k}\mathbf{x}}$, where $V = L^d$ is the volume of the system, d is the spatial dimensionality, and Λ is the upper cut-off of the wave vectors. The Fourier-transformed Hamiltonian obeys the equation

$$\begin{aligned} -\frac{H}{T} &= -\frac{1}{2} \sum_{i,\mathbf{k}} (r + c\mathbf{k}^2) |\varphi_{i,\mathbf{k}}|^2 \\ &- \frac{1}{8} V^{-1} \sum_{i,j,\mathbf{k}_1,\mathbf{k}_2,\mathbf{k}_3} \varphi_{i,\mathbf{k}_1} \varphi_{i,\mathbf{k}_2} u_{\mathbf{k}_1+\mathbf{k}_2} \varphi_{j,\mathbf{k}_3} \varphi_{j,-\mathbf{k}_1-\mathbf{k}_2-\mathbf{k}_3}. \end{aligned} \quad (2)$$

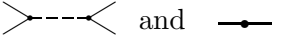
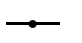
In the Feynman diagram technique [2, 12], the second term in (2) is represented by a fourth order vertex  (where field components with vanishing total wave vector are related to the solid lines and the remaining factor — to the dashed line). In the following we will consider only a particular case $u(\mathbf{x}) = u\delta(\mathbf{x})$ or $u_{\mathbf{k}} = u$. The fourth order vertex then can be depicted as  by shrinking the dashed line to a point (node). We will mostly use this simplified notation. One has to remember, however, that two of the vertex lines are related to i -th component ($i = 1, \dots, n$), and the other two lines — to j -th component of a field vector (including the possibility $i = j$). It is shown explicitly in the representation , where these pairs of lines are separated.

In the exact Wilson’s RG equation the scale transformation, i. e., the Kadanoff’s transformation, is performed by integrating over the Fourier modes with wave vectors obeying $\Lambda/s < k < \Lambda$.

It is the first step of the full RG transformation. At this step the transformed Hamiltonian H' is found from the equation

$$e^{-(H'/T)+AL^d} = \int e^{-H/T} \prod_{i, \Lambda/s < k < \Lambda} d\varphi_{i,\mathbf{k}}, \quad (3)$$

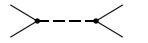
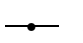
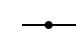
where A is a constant. Note that $\varphi_{i,\mathbf{k}}$ is a complex number and $\varphi_{i,-\mathbf{k}} = \varphi_{i,\mathbf{k}}^*$ holds (since $\varphi_i(\mathbf{x})$ is always real), so that the integration over $\varphi_{i,\mathbf{k}}$ in (3) means in fact the integration over real and imaginary parts of $\varphi_{i,\mathbf{k}}$ for each pair of conjugated wave vectors \mathbf{k} and $-\mathbf{k}$. In practice Eq. (3) cannot be solved exactly. It is done perturbatively, as described in [2]. The perturbation terms can be found more easily by means of the Feynman diagrams.

In the perturbative approach, Hamiltonian is split in two parts $H = H_0 + H_1$, where H_0 is the Gaussian part and H_1 is the rest part considered as a small perturbation. The first and the second term on the right hand side of (2) can be identified with $-H_0/T$ and $-H_1/T$, respectively. Since the term with r also is considered as a small perturbation ($r \sim \varepsilon$ holds in the ε -expansion in $d = 4 - \varepsilon$ dimensions), it is suitable to include it in H_1 . In this case diagram expansions are represented by vertices  and , where the latter second-order vertex corresponds to the term with r .

It is convenient to normalize Eq. (3) by $Z_s = \int \exp(-\tilde{H}_0/T) \prod_{i, \Lambda/s < k < \Lambda} d\varphi_{i,\mathbf{k}}$, where \tilde{H}_0 is the part of H_0 including only the terms with $\Lambda/s < k < \Lambda$. We have $\ln Z_s = A_s L^d$ at $L \rightarrow \infty$, where A_s is independent of L , and the normalization yields

$$-(H'/T) + (A - A_s)L^d = -(H'_0/T) + \ln \langle \exp(-H_1/T) \rangle_0, \quad (4)$$

where $\langle \cdot \rangle_0$ means the Gaussian average over the field components with $\Lambda/s < k < \Lambda$, whereas H'_0 is the part of H_0 including only the components with $k < \Lambda/s$. Like free energy, $\ln \langle \exp(-H_1/T) \rangle_0$ is represented perturbatively by the sum over all connected Feynman diagrams made of the vertices of $-H_1/T$ by coupling those solid lines, which are associated with wave vectors obeying $\Lambda/s < k < \Lambda$, according to the Wick's theorem. A diagram can contain no coupled lines. There is also a set of diagrams with all lines coupled. The latter diagrams give a constant (independent of $\varphi_{i,\mathbf{k}}$) contribution which compensates the term $(A - A_s)L^d$ in (4). The other contributions correspond to $-H'/T$.

Each term of $\ln \langle \exp(-H_1/T) \rangle_0$ comes from a diagram (or diagrams) of certain topology and is given by a sum over wave vectors which fulfil certain constraints such that $k < \Lambda/s$ holds for uncoupled (external or outer) solid lines, associated with field components $\varphi_{i,\mathbf{k}}$, and $\Lambda/s < k < \Lambda$ holds for coupled solid lines. Besides, the sum of all wave vectors coming into any of the nodes is zero, and the same index i is related to the solid lines attached to one node of any vertex  or . The Gaussian average $G_0(\mathbf{k}) = \langle \varphi_{i,\mathbf{k}} \varphi_{i,-\mathbf{k}} \rangle_0 = \langle |\varphi_{i,\mathbf{k}}|^2 \rangle_0$ is related to a coupling line with wave vector \mathbf{k} . Here $G_0(\mathbf{k})$ is the Fourier transform of the two-point correlation function in the Gaussian approximation. If only the term with \mathbf{k}^2 in (2) is included in H_0/T , then we have $G_0(\mathbf{k}) = 1/(ck^2)$. Including also the term with r , we have $G_0(\mathbf{k}) = 1/(r + ck^2)$, but in this case we need finally to expand $G_0(\mathbf{k})$ in terms of r . The second method yields the same results as the first one: such an expansion generates the same terms, which are obtained in the first method by extending coupling lines in the diagrams originally constructed without vertices  to include all possible linear chains made of these vertices. We will use the first, i. e., more diagrammatic method. Note that, when the renormalization procedure is repeated, a continuum of additional vertices appear in the expansion of $-H_1/T$,



including ones with explicit wave-vector dependent factors related to the solid lines, which then also have to be taken into account.

In fact, the first step of RG transformation implies the summation over wave vectors of the coupled lines in the diagrams, resulting in a Hamiltonian which depends on $\varphi_{i,\mathbf{k}}$ with $k < \Lambda/s$. The RG transformation has the second step [2]: changing of variables $\tilde{\mathbf{k}} = s\mathbf{k}$ and rescaling the field components $\varphi_{i,\mathbf{k}} \rightarrow s^{1-\eta/2}\varphi_{i,\tilde{\mathbf{k}}}$, where η is the critical exponent describing the $\sim k^{-2+\eta}$ singularity of the Fourier-transformed critical two-point correlation function at $k \rightarrow 0$. The upper cut-off for the new wave vectors $\tilde{\mathbf{k}}$ is the original one Λ , whereas the density of points in the $\tilde{\mathbf{k}}$ -space corresponds to s^d times decreased volume. Therefore we make a substitution $\tilde{V} = s^{-d}V$. In the thermodynamic limit we can replace \tilde{V} by V consistently increasing the density of points in the wave vector space. Finally, we set $\tilde{\mathbf{k}} \rightarrow \mathbf{k}$ and obtain a Hamiltonian in original notations.

3 Renormalization up to the order of ε^2

3.1 RG flow equations


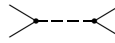
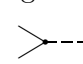
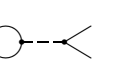
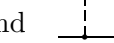
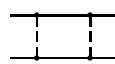
Here we consider RG flow equations including all terms up to the order $\mathcal{O}(\varepsilon^2)$, starting with the renormalization of the coupling constant u . In fact, this is the lowest order of the theory, since it allows to find the fixed point value u^* up to the order of ε . Our aim is to show that we can easily recover the known results using the diagrammatic approach described in Sec. 2. It allows also to write down unambiguously (i. e., without intermediate approximations) the formulae for all perturbation terms.

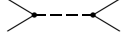
Important statements here are that the renormalized values of r and u are quantities of order $\mathcal{O}(\varepsilon)$. Besides, $\eta = \mathcal{O}(\varepsilon^2)$ holds within the ε -expansion and, for any finite renormalization scale s , the variation of c is of order $\mathcal{O}(\varepsilon^2)$ [2]. Hence, performing the RG transformation R_s with a finite s , the only diagrams of $\ln\langle\exp(-H_1/T)\rangle_0$ contributing to the renormalized coupling constant up to the order of ε^2 are  (this statement can be verified in detail based on a complete renormalization discussed further on). The first one provides the original φ^4 term in Eq. (2), which is merely renormalized by factor $s^{\varepsilon-2\eta}$ at the second step of the RG transformation. The second diagram, which is constructed of two vertices , yields

$$\begin{aligned} \text{Diagram} &\rightarrow s^{\varepsilon-2\eta} \left(\frac{u}{8c}\right)^2 V^{-1} \sum_{i,j,\mathbf{k}_1,\mathbf{k}_2,\mathbf{k}_3} \varphi_{i,\mathbf{k}_1} \varphi_{i,\mathbf{k}_2} \varphi_{j,\mathbf{k}_3} \varphi_{j,-\mathbf{k}_1-\mathbf{k}_2-\mathbf{k}_3} \times \\ &\times [(4n+16)Q((\mathbf{k}_1+\mathbf{k}_2)/s,s) + 16Q((\mathbf{k}_1+\mathbf{k}_3)/s,s)]. \end{aligned} \quad (5)$$

Here Q is given by

$$Q(\mathbf{k},s) = \frac{1}{(2\pi)^d} \int_{\Lambda/s < q < \Lambda} q^{-2} |\mathbf{k}-\mathbf{q}|^{-2} \mathcal{F}(|\mathbf{k}-\mathbf{q}|,s) d^d q, \quad (6)$$

where $\mathcal{F}(k,s) = 1$ if $\Lambda/s < k < \Lambda$, and $\mathcal{F}(k,s) = 0$ otherwise. To obtain this result, we have deciphered the  diagram as a sum of three diagrams of different topologies made of vertices , i. e., , , and , providing the same topological picture  when shrinking the dashed lines to points. Note that any

loop made of solid lines of  gives a factor n , and one needs also to compute the combinatorial factors (see, e. g., [2, 12]). For the above three diagrams, the resulting factors are $4n$, 16 , and 16 , which enter the pre-factors of Q in (5).

Quantity $Q(\mathbf{k}/s, s)$ has a constant contribution


$$Q(\mathbf{0}, s) = K_d \Lambda^{-\varepsilon} (s^\varepsilon - 1)/\varepsilon, \quad (7)$$

as well as a \mathbf{k} -dependent correction $\Delta(k, s) = Q(\mathbf{k}/s, s) - Q(\mathbf{0}, s)$ vanishing at $k = 0$. Here $K_d = S(d)/(2\pi)^d$, where $S(d) = 2\pi^{d/2}/\Gamma(d/2)$ is the area of unit sphere in d dimensions.

The term provided by the $Q(\mathbf{0}, s)$ part of $Q(\mathbf{k}/s, s)$ in (5) is identified with the φ^4 vertex, contributing to the renormalized coupling constant u' . It is consistent with the general form

$$V^{-1} \sum_{i,j,\mathbf{k}_1,\mathbf{k}_2,\mathbf{k}_3} \bar{Q}(\mathbf{k}_1, \mathbf{k}_2, \mathbf{k}_3, s, n, \varepsilon) \varphi_{i,\mathbf{k}_1} \varphi_{i,\mathbf{k}_2} \varphi_{j,\mathbf{k}_3} \varphi_{j,-\mathbf{k}_1-\mathbf{k}_2-\mathbf{k}_3}, \quad (8)$$

of quartic (φ^4) terms, where the contribution corresponding to the ordinary φ^4 vertex is uniquely identified with one provided by the constant part $\bar{Q}(\mathbf{0}, \mathbf{0}, \mathbf{0}, s, n, \varepsilon)$ of the weight function \bar{Q} .

Taking into account also the contribution coming directly from  vertex, the RG flow equation reads

$$u' = s^{\varepsilon-2\eta} \left[u - u^2 \frac{K_d(n+8)}{2c^2 \Lambda^\varepsilon} \times \frac{s^\varepsilon - 1}{\varepsilon} \right] + \mathcal{O}(\varepsilon^3), \quad (9)$$

where u' is the renormalized and u is the original coupling constant. The expansion in ε yields the well known equation [2]

$$u' = u + \varepsilon u \ln s - u^2 B \ln s + \mathcal{O}(\varepsilon^3), \quad (10)$$

where $B = K_d(n+8)/(2c^2)$, with the known fixed-point value at $u = u^* = B^{-1}\varepsilon + \mathcal{O}(\varepsilon^2)$.


The correction term $\Delta(k, s)$ changes the renormalized Hamiltonian as follows:

$$\begin{aligned} H/T \rightarrow (H/T) - s^{\varepsilon-2\eta} \left(\frac{u}{2c} \right)^2 V^{-1} \sum_{i,j,\mathbf{k}_1,\mathbf{k}_2,\mathbf{k}_3} \varphi_{i,\mathbf{k}_1} \varphi_{i,\mathbf{k}_2} \varphi_{j,\mathbf{k}_3} \varphi_{j,-\mathbf{k}_1-\mathbf{k}_2-\mathbf{k}_3} \times \\ \times [(1+n/4) \Delta(|\mathbf{k}_1 + \mathbf{k}_2|, s) + \Delta(|\mathbf{k}_1 + \mathbf{k}_3|, s)]. \end{aligned} \quad (11)$$

It can be represented as a sum of two fourth-order vertices including pre-factors $\Delta(|\mathbf{k}_1 + \mathbf{k}_2|, s)$ and $\Delta(|\mathbf{k}_1 + \mathbf{k}_3|, s)$, respectively, related to two of the vertex lines.

In the following we will introduce a more suitable diagrammatic notation. In the one-component case $n = 1$, the term appearing in (5) is represented as

$$s^{2\varepsilon-2\eta} \frac{9}{16} u^2 \text{ > } \text{---} \text{---} \text{---} \text{---} \text{ <} \quad (12)$$

where  is the Feynman diagram in which the Gaussian propagator $1/(ck^2)$ with $k \in [\Lambda, s\Lambda]$ is related to the dotted coupling lines. In other words, the propagator is multiplied with the cut function $\mathcal{F}(k/s, s)$. In general (also for other diagrams considered in our paper), the field components supplied with the factor V^{1-m} are related to $2m$ external lines, the rest of such factors being absorbed in the \mathbf{k} -space integrals. An additional s^ε factor in (12) comes from the rescaling of wave vectors in such a way that the integration now takes place over $k \in [\Lambda, \Lambda s]$

in a process of repeated renormalization. Here ζ is the previous and ζ' is the new (renormalized) value of this parameter after the current RG transformation (RGT) with the scale factor s . The weight coefficients a_4 and a_6 in this order of the ε -expansion obey simple RG flow equations

$$a'_4 = -\frac{9u^2}{16} + \mathcal{O}(\varepsilon^3) \quad (19)$$

$$a'_6 = -\frac{u^2}{8} + \mathcal{O}(\varepsilon^3) \quad (20)$$

relating the new values of these parameters in each RGT to the previous value of u . The initial values of a_4 and a_6 are not important, since the corresponding diagrams vanish at $\zeta = 1$. The RG flow equations for the Hamiltonian parameters u and r read

$$u' = s^\varepsilon \left[u - \frac{n+8}{2} u^2 \mathbf{0} \text{---} \text{---} \right] + \mathcal{O}(\varepsilon^3) \quad (21)$$

$$r' = s^2 \left[\left(r + \frac{n+2}{2} u \mathbf{0} \text{---} \text{---} \right) \left(1 - \frac{n+2}{2} u \mathbf{0} \text{---} \text{---} \right) - \frac{n+2}{2} \left(u^2 \mathbf{0} \text{---} \text{---} - \frac{16}{3} a_4 \mathbf{0} \text{---} \text{---} - 24a_6 \mathbf{0} \text{---} \text{---} \right) \right] + \mathcal{O}(\varepsilon^3), \quad (22)$$

where $\mathbf{0} \text{---} \text{---}$ is the diagram with amputated four external lines having zero wave vectors, and the other diagrams are defined analogously. The wave vectors of the internal solid lines are in the range $[\Lambda/s, \Lambda]$, whereas those of the dotted lines — in the range $[\Lambda, \Lambda\zeta]$. Eq. (21) is the same as (9), only the irrelevant for this order of the ε -expansion factor $s^{-2\eta}$ is omitted, like also the factor $s^{-\eta}$ in (22). Taking into account (19)–(20) and the fact that u is renormalized only by $\mathcal{O}(\varepsilon^2)$ in one RGT, the diagram expression in the last line of (22) can be written as $-\frac{1}{2}(n+2)u^2 \left(\mathbf{0} \text{---} \text{---} + 3 \mathbf{0} \text{---} \text{---} + 3 \mathbf{0} \text{---} \text{---} \right)$.

The parameter c enters all diagrams. In the actual order of the ε -expansion its variation does not produce additional terms in (21) and (22). However, one has to update its value according to the equation

$$c' = s^{-\eta} \left(c - \frac{n+2}{2} \Pi \right) + \mathcal{O}(\varepsilon^3), \quad (23)$$

where

$$\Pi = \lim_{k \rightarrow 0} \frac{D(k) - D(0)}{k^2} \quad (24)$$

with

$$D(k) = u^2 \left(\mathbf{k} \text{---} \text{---} + 3 \mathbf{k} \text{---} \text{---} + 3 \mathbf{k} \text{---} \text{---} \right). \quad (25)$$

It is true if the limit (24) exists. Here the symbol \mathbf{k} indicates the wave vector related to the amputated external line. Finally, the RG flow equation for the function $\theta(\mathbf{k})$ reads

$$\theta'(\mathbf{k}) = s^2 \left(\theta(\mathbf{k}/s) - \frac{n+2}{2} \Phi(\mathbf{k}/s) \right) + \mathcal{O}(\varepsilon^3), \quad (26)$$

where

$$\Phi(\mathbf{k}) = D(k) - D(0) - k^2 \Pi. \quad (27)$$

Using the diagram technique, the function $\theta(\mathbf{k})$ can be represented as

$$\theta(\mathbf{k}) = -\frac{n+2}{2}u^2 \mathbf{k} \text{ (wavy line)} + \mathcal{O}(\varepsilon^3) , \quad (28)$$

where the wavy line indicates that both the constant contribution and that proportional to k^2 (with the proportionality coefficient determined at $k \rightarrow 0$) are subtracted. Besides, the range of the wave vectors for the internal lines is $[\Lambda, \Lambda\zeta]$, where ζ is determined after the actual RGT.

A question can arise about the existence of the limit (24). In fact, it is a necessary condition for the stability of the RG flow that a finite (or zero) limit in (24) exists. It can be shown directly that it exists for $s = 1 + ds$ with small ds and $\zeta = \infty$ (see Sec. 6.4.3), as well as at small ds and $\zeta = 1 + d\zeta$ with small $d\zeta$. Besides, the limit exists for each diagram separately in this case. Consequently, the limit (24) exists at least at the beginning of the renormalization process, performed in small steps. In this paper we will test several important properties, in the case if the limit (24) exists for any finite $s > 1$. Besides, we will test the scenario, where this limit exists separately for the first diagram in (25) and for the sum of the remaining two diagrams. These, in fact, are conditions at which a set of expected properties hold, as shown further on.

3.2 Proof of the RG flow equations

In Sec. 3.1 the RG flow equations are given without proof. Their proof consists of a verification that, at each RGT, the Hamiltonian keeps the form (17) in accordance with the given update rules for all parameters. Consider first the φ^6 vertex at $n = 1$, summing up all diagrams of this topology, which appear in H/T at a given RGT:

$$\begin{aligned} s^{2\varepsilon-3\eta} \left(-\frac{u^2}{8} \text{ (solid)} + a_6 \text{ (dashed)} \right) &= -\frac{u^2}{8} \left(\text{ (solid)} + \text{ (dashed)} \right) + \mathcal{O}(\varepsilon^3) \\ &= -\frac{u^2}{8} \text{ (dotted)} + \mathcal{O}(\varepsilon^3) = a'_6 \text{ (dotted)} + \mathcal{O}(\varepsilon^3) . \end{aligned} \quad (29)$$

Here the wave vectors within $[\Lambda, \Lambda s]$, $[\Lambda s, \Lambda\zeta']$, and $[\Lambda, \Lambda\zeta']$ correspond to the solid, dashed, and dotted coupling lines, respectively, where $\zeta' = s\zeta$. (These dashed lines should not be confused with those of $\text{ (dashed)} .$) In (29), the vertex (solid) is produced by coupling (and rescaling) two φ^4 vertices (cross) , whereas (dashed) comes from the rescaling of already existing before the given RGT φ^6 vertex. We have omitted the irrelevant for this order of the ε -expansion rescaling factor resulting from the renormalization of parameter c . We have used the substitution $a_6 = -u^2/8 + \mathcal{O}(\varepsilon^3)$, which holds according to the assumption that our RG flow equation (20) was satisfied and u was changed only by $\mathcal{O}(\varepsilon^2)$ in the previous RGT. It is true for the first RGT, so that the relations (29) provide the proof of (20) by induction. It is obviously valid for any finite number of RGT.

The generalisation to the n -component case is trivial here, since there is only one way how to couple two vertices (dashed) to form the sixth-order vertex.

Similarly, the summation of terms provided by the diagrams of (loop) topology, subtracting the contribution included in the ordinary φ^4 vertex, gives us

$$s^{2\varepsilon-2\eta} \left(-\frac{9u^2}{16} \text{ (loop)} + a_4 \text{ (cross)} + 9a_6 \text{ (loop)} \right)$$

$$\begin{aligned}
&= -\frac{9u^2}{16} \left(\text{diag}_1 + \text{diag}_2 + 2 \text{diag}_3 \right) + \mathcal{O}(\varepsilon^3) \\
&= -\frac{9u^2}{16} \text{diag}_4 + \mathcal{O}(\varepsilon^3) = a'_4 \text{diag}_4 + \mathcal{O}(\varepsilon^3)
\end{aligned} \tag{30}$$

with the same k intervals for different coupling lines as in (29). It proves (19) for a finite number m of RG transformations at $n = 1$. Here the three diagrams in the first line of (30) come from two \times vertices, rescaling of the already existing vertex with the coefficient a_4 , and from the φ^6 vertex via coupling its two lines. Besides, $\text{diag}_1 \equiv \text{diag}_3$ holds, since the diagram diag_1 vanishes if the external lines have zero wave vectors. This derivation is easily generalised to the n -component case represented by (17): the same relations, only multiplied with the corresponding weight factors in (14), hold for diagrams of each topology, when diag_4 is deciphered as the diagrams on the right hand side of (14).

The derivation of (21) has been already discussed in Sec. 3.1. Recall that the updated value of the coupling constant u of the ordinary φ^4 vertex is related to the constant part of the weight function in (8), which comes from the rescaled already existing ordinary φ^4 vertex, as well as from other diagrams with four external lines generated in the actual RGT. The coupling of two lines of the vertex diag_4 gives vanishing contribution here, so that the coupling diag_1 is the only relevant one at the order of ε^2 . It results in (21).

Similarly, the updated value of the parameter r is identified with the constant part of the weight function $\tilde{\theta}(\mathbf{k})$ in the general representation of the quadratic term $(1/2) \sum_{i,\mathbf{k}} \tilde{\theta}(\mathbf{k}) |\varphi_{i,\mathbf{k}}|^2$, and is generated by the diagrams with two external lines. It results in (22), where the terms with a_4 and a_6 appear via coupling the lines of the vertices diag_4 and diag_5 , respectively, whereas other diagrams in (22) are produced by the vertices \times and \bullet .

The RG flow equation (23) for the parameter c is similar to that for r with the only difference that here we single out the contribution to $\tilde{\theta}(\mathbf{k})$, which is proportional to k^2 . Subtracting both the constant contribution and that of k^2 , we arrive at the equation for $\theta(\mathbf{k})$ (26). Its diagrammatic form (28) is proven by summation of diagrams like, e. g., in Eq. (30).

Finally, we check that all terms up to the order of ε^2 are already included. In particular, the part of (17) with factor $\theta(\mathbf{k})/2$ can be seen as the vertex \bullet supplied with such a weight factor. However, its coupling to other vertices gives only a contribution of order $\mathcal{O}(\varepsilon^3)$. Recall that we do not consider the constant part of Hamiltonian, which is independent of the field configuration and is represented by closed diagrams without external lines.

3.3 Estimation of \mathbf{k} -space integrals

It is important to know whether the \mathbf{k} -space integrals over the internal lines of the diagrams, appearing in our representation of the renormalized Hamiltonian, are convergent when the RG transformation is repeated unlimitedly many times, i. e., at $\zeta \rightarrow \infty$.

First, we note that the diagram \bullet in four dimensions, i. e.,

$$\bullet = \frac{1}{(2\pi)^4} \int_{\Lambda < q < \Lambda\zeta} \frac{d^4q}{c^2 q^4} = \frac{K_4}{c^2} \int_{\Lambda}^{\Lambda\zeta} \frac{dq}{q} = \frac{K_4}{c^2} \ln \zeta \tag{31}$$

diverges when the region $q \in [\Lambda, \Lambda\zeta]$ of wave vectors for the internal lines is extended to $[\Lambda, \infty]$ at $\zeta \rightarrow \infty$. Similar diagram, where the zero- \mathbf{k} contribution is subtracted,

$$J(k, \zeta) = \text{diagram with } \mathbf{k} \text{ and } \zeta \text{ lines} = \text{diagram with } \mathbf{k} \text{ and } \zeta \text{ lines} - \text{diagram with } \mathbf{0} \text{ and } \zeta \text{ lines} \quad (32)$$

with \mathbf{k} corresponding to the sum of wave vectors for the two amputated external lines, is convergent at $d = 4$, as well as in $d = 4 - \varepsilon$ dimensions, where we have

$$\begin{aligned} J(q, \zeta) &= \frac{1}{c^2(2\pi)^d} \int_{\Lambda < k < \Lambda\zeta} \left(\frac{\hat{\mathcal{F}}(|\mathbf{q} + \mathbf{k}|, \zeta)}{k^2 |\mathbf{q} + \mathbf{k}|^2} - \frac{1}{k^4} \right) d^d k \\ &= \frac{K_d}{c^2 \int_0^\pi (\sin \theta)^{2-\varepsilon} d\theta} \times \int_{\Lambda}^{\Lambda\zeta} k^{1-\varepsilon} dk \int_0^\pi \left(\frac{\hat{\mathcal{F}}(\sqrt{q^2 + 2kq \cos \theta + k^2}, \zeta)}{q^2 + 2kq \cos \theta + k^2} - \frac{1}{k^2} \right) (\sin \theta)^{2-\varepsilon} d\theta \end{aligned} \quad (33)$$

with $\hat{\mathcal{F}}(k, \zeta) = 1$ if $\Lambda < k < \Lambda\zeta$, and $\hat{\mathcal{F}}(k, \zeta) = 0$ otherwise. The last identity in (33) is true for any integer $d \geq 2$, according to the well known formula for integration in spherical coordinates, so that we can put here ε as a continuous parameter in the usual sense of the ε -expansion.

In the following calculations of this subsection, we set $c = 1$ and $\Lambda = 1$ for simplicity. Considering the large- q asymptotic at $\zeta = \infty$, we can set $\hat{\mathcal{F}} = 1$ in (33), which gives correct result up to a term vanishing at $q \rightarrow \infty$. Further on, we use the decomposition

$$\frac{1}{k^2 |\mathbf{q} + \mathbf{k}|^2} - \frac{1}{k^4} = f_0(k, q) + \Delta f(\mathbf{k}, \mathbf{q}), \quad (34)$$

where

$$f_0(k, q) = \begin{cases} k^{-2}q^{-2} - k^{-4} & , \quad k < q \\ 0 & , \quad k > q \end{cases} \quad (35)$$

An important property of $\Delta f(\mathbf{k}, \mathbf{q})$, defined by (34) and (35), is

$$\int_{k>1} \Delta f(\mathbf{k}, \mathbf{q}) d^4 k = 0 \quad \text{at } q \rightarrow \infty. \quad (36)$$

It is true because

$$\frac{1}{(2\pi)^4} \int_{k>1} \left(\frac{1}{k^2 |\mathbf{q} + \mathbf{k}|^2} - \frac{1}{k^4} \right) d^4 k = \frac{1}{(2\pi)^4} \int_{k>1} f_0(k, q) d^4 k = -\ln q + \frac{1}{2} \quad (37)$$

holds at $q \rightarrow \infty$. The $-\ln q + 1/2$ asymptotic is evident for the second integral. For the first one, it is verified by integration over k (via the substitution $p = k + q \cos \theta$) and then – over the angle θ in spherical coordinates. According to the decomposition (34), we have

$$J(q, \infty) = K_d \left\{ \frac{q^{-\varepsilon}}{2-\varepsilon} - \frac{1-q^{-\varepsilon}}{\varepsilon} \right\} + \Delta J(q) \quad \text{at } q \rightarrow \infty, \quad (38)$$

where the term $K_d \{\cdot\}$ is the contribution of $f_0(k, q)$, whereas $\Delta J(q)$ comes from $\Delta f(\mathbf{k}, \mathbf{q})$ and is equal to

$$\Delta J(q) = \frac{K_d \Gamma[(4-\varepsilon)/2]}{\sqrt{\pi} \Gamma[(3-\varepsilon)/2]} \times \int_1^\infty k^{-1-\varepsilon} dk \int_0^\pi \Delta \tilde{f}(k/q, \theta) (\sin \theta)^{2-\varepsilon} d\theta, \quad (39)$$

where

$$\Delta \tilde{f}(x, \theta) = \frac{x^2}{1 + 2x \cos \theta + x^2} - 1 + (1 - x^2) \Theta(1 - x) . \quad (40)$$

Here $\Theta(x)$ denotes the theta step function, and the known identity

$$\int_0^\pi (\sin \theta)^x d\theta = \sqrt{\pi} \frac{\Gamma\left(\frac{x+1}{2}\right)}{\Gamma\left(\frac{x+2}{2}\right)} \quad (41)$$

has been used to obtain (39). According to (36), $\Delta J(q)$ vanishes at $d = 4$. Using this property, from (39) we obtain

$$\Delta J(q) = \frac{2}{\pi} K_d \mathcal{A} \left(-\varepsilon + \varepsilon^2 \ln q \right) + \tilde{c} \varepsilon^2 + \mathcal{O}(\varepsilon^3) , \quad (42)$$

where

$$\mathcal{A} = \int_0^\infty \frac{\ln x}{x} dx \int_0^\pi \Delta \tilde{f}(x, \theta) \sin^2 \theta d\theta + \int_0^\infty \frac{dx}{x} \int_0^\pi \Delta \tilde{f}(x, \theta) \sin^2 \theta \ln(\sin \theta) d\theta \quad (43)$$

and \tilde{c} is a constant at $q \rightarrow \infty$. According to (38) and (42), we have

$$\begin{aligned} J(q, \infty) &= K_d \left[-\ln q + \frac{1}{2} + \frac{\varepsilon}{2} \left(\ln^2 q - \ln q \right) + \left(\frac{1}{4} - \frac{2\mathcal{A}}{\pi} \right) \left(\varepsilon - \varepsilon^2 \ln q \right) \right. \\ &\quad \left. + \frac{\varepsilon^2}{12} \left(-2 \ln^3 q + 3 \ln^2 q \right) + \hat{c} \varepsilon^2 \right] + \mathcal{O}(\varepsilon^3) \quad \text{at } q \rightarrow \infty , \end{aligned} \quad (44)$$

where \hat{c} is a constant.

In a more general case, for $J(q, \zeta)$ we obtain


$$J(q, \zeta) = J(q, \infty) + \delta J(q, \zeta) , \quad (45)$$

where $\delta J(q, \zeta)$ has the asymptotic form

$$\delta J(q, \zeta) = q^{-\varepsilon} \hat{f}(\zeta/q, \varepsilon) \quad \text{at } q, \zeta \rightarrow \infty , \quad (46)$$

where

$$\begin{aligned} \hat{f}(y, \varepsilon) &= -\frac{K_d \Gamma[(4 - \varepsilon)/2]}{\sqrt{\pi} \Gamma[(3 - \varepsilon)/2]} \left\{ \int_0^y x^{-1-\varepsilon} dx \int_0^\pi \frac{x^2 \Theta(1 + 2x \cos \theta + x^2 - y^2)}{1 + 2x \cos \theta + x^2} (\sin \theta)^{2-\varepsilon} d\theta \right. \\ &\quad \left. + \int_y^\infty x^{-1-\varepsilon} dx \int_0^\pi \left(\frac{x^2}{1 + 2x \cos \theta + x^2} - 1 \right) (\sin \theta)^{2-\varepsilon} d\theta \right\} . \end{aligned} \quad (47)$$

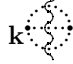
Based on these results, we can evaluate the large- \mathbf{q} (i. e., $C < q < \zeta$ for large enough C at a given k) contribution to the diagram  in four dimensions as



$$\frac{1}{(2\pi)^4} \int_{C < q < \zeta} [J(|\mathbf{k} + \mathbf{q}|, \zeta) - J(q, \zeta)] q^{-2} d^4 q . \quad (48)$$

It, in fact, diverges at $\zeta \rightarrow \infty$, and the divergent part comes from the $-K_4 \ln q$ term in $J(q, \infty)$, providing the contribution

$$-\frac{K_4^2}{\pi} \int_C^\zeta q dq \int_0^\pi \ln \left(1 + \frac{2kq \cos \theta + k^2}{q^2} \right) \sin^2 \theta d\theta . \quad (49)$$

Using the expansion in powers of k/q , we see that (49) logarithmically diverges at $\zeta \rightarrow \infty$. However, if we subtract the term $\propto k^2$, the result is convergent. It indicates that the diagram

 in (28) has finite value at $\zeta \rightarrow \infty$.

Similarly, we can treat the large-wave-vector contribution to the diagram  further considered in the renormalization up to the order of ε^3 . This graph contains the subtraction of the zero-vector contribution from the internal block , as well as from the whole diagram. It is defined (at $c = \Lambda = 1$) by

$$\text{Diagram} = \frac{1}{(2\pi)^4} \int_{1 < q_1 < \zeta} \left\{ q_1^{-2} | \mathbf{q}_1 + \mathbf{k} |^{-2} \hat{\mathcal{F}}(| \mathbf{q}_1 + \mathbf{k} |, \zeta) J(| \mathbf{q} - \mathbf{q}_1 |, \zeta) - q_1^{-4} J(q_1, \zeta) \right\} d^4 q_1 \quad (50)$$

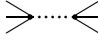
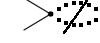
in four dimensions. Using the asymptotic estimates of $J(q, \infty)$ and $\delta J(q, \zeta)$, we find that the tail of large q_1 is convergent for any given \mathbf{k} and \mathbf{q} .

The actual integrals (49) and (50) have been estimated in four dimensions ($d = 4$). Those ones, which are convergent at $d = 4$, are convergent also in $d = 4 - \varepsilon$ dimensions for small (positive and also negative) ε when considering the \mathbf{k} -space integrals as continuous functions of d in the usual sense of the ε -expansion. It is because the contribution of large wave vectors changes only slightly.

3.4 Testing the semigroup property

Here we test the semigroup property

$$R_{s_1 s_2} \mu = R_{s_2} R_{s_1} \mu \quad (51)$$

discussed already in Sec. 1. In fact, we verify that the renormalized Hamiltonian after two subsequent RGT with scale factors s_1 and s_2 is the same as after one RGT with the scale factor $s_1 s_2$. It can be seen most easily for the vertices  and , as consistent with Eqs. (18) to (20) and the fact that u is renormalized only by an amount of $\mathcal{O}(\varepsilon^2)$. The semigroup property for the coupling constant u easily follows from (21). After the first RGT we have

$$u' = s_1^\varepsilon \left[u - \frac{n+8}{2} u^2 \text{Diagram} \right] + \mathcal{O}(\varepsilon^3) , \quad (52)$$

where the dotted line refers to the k interval $[\Lambda/s_1, \Lambda]$. After the second RGT the value of the coupling constant, denoted as u'' , becomes

$$u'' = s_2^\varepsilon \left[u' - \frac{n+8}{2} u'^2 s_1^{-\varepsilon} \text{Diagram} \right] + \mathcal{O}(\varepsilon^3) , \quad (53)$$

where the dashed line refers to the interval $[\Lambda/(s_1 s_2), \Lambda/s_1]$. Here the rescaling of the wave vectors from $k \in [\Lambda/s_2, \Lambda]$ to $k \in [\Lambda/(s_1 s_2), \Lambda/s_1]$ has been performed for convenience. Inserting (52) in (53), and taking into account that $u = \mathcal{O}(\varepsilon)$, we obtain

$$\begin{aligned} u'' &= (s_1 s_2)^\varepsilon \left[u - \frac{n+8}{2} u^2 \left\{ \mathbf{0} \begin{array}{c} \cdots \\ \cdots \end{array} + \mathbf{0} \begin{array}{c} \dashrightarrow \\ \dashleftarrow \end{array} \right\} \right] + \mathcal{O}(\varepsilon^3) \\ &= (s_1 s_2)^\varepsilon \left[u - \frac{n+8}{2} u^2 \mathbf{0} \begin{array}{c} \circ \\ \circ \end{array} \right] + \mathcal{O}(\varepsilon^3) , \end{aligned} \quad (54)$$

where $k \in [\Lambda/(s_1 s_2), \Lambda]$ corresponds to the solid coupling lines. It is obvious that (54) is identical to the result of one RGT obtained from (21) with $s = s_1 s_2$, which proves the semigroup property. Analogous diagram summation proves this property also in the next order of the ε -expansion [13].

The semigroup property for the parameter r , when performing the RG transformations of the initial Hamiltonian with $\zeta = 1$, is proven straightforwardly by the same method. Namely, the result of the second RGT (applying (22)) is represented by the diagrams containing the dotted and the dashed lines with $k \in [\Lambda/s_1, \Lambda]$ and $k \in [\Lambda/(s_1 s_2), \Lambda/s_1]$, respectively. These diagrams sum up to give ones with $k \in [\Lambda/(s_1 s_2), \Lambda]$, which correspond to those of the one-step renormalization with $s = s_1 s_2$. In distinction to the case of u , here more complicated terms appear, including different lines in one diagram. The situation is less trivial when starting with $\zeta > 1$. In this case all diagrams can be decomposed in such ones, which contain three types of lines with $k \in [\Lambda, \Lambda\zeta]$, $k \in [\Lambda/s_1, \Lambda]$ and $k \in [\Lambda/(s_1 s_2), \Lambda/s_1]$, respectively. Then we prove the semigroup property by checking that such diagram representation for the two-step renormalization is identical (up to the considered order of the ε -expansion) to that for the one-step renormalization. The semigroup property for the parameters c and $\theta(\mathbf{k})$ is proven by this method, as well.

3.5 The fixed point


The RG flow described by the truncated perturbative equations of Sec. 3.1 has certain fixed point as a steady state solution of the RG flow equations. We shall mark the fixed-point values by an asterisk, except the value of c , since the fixed point exists for any given c , as it will be seen from the following analysis. The fixed-point value of the coupling constant u , i. e.,

$$u^* = \frac{2c^2}{(n+8)K_4} \varepsilon + \mathcal{O}(\varepsilon^2) \quad (55)$$

has been already mentioned in Sec. 3.1. According to (19) and (20), we have $a_4^* = -(9u^{*2})/16 + \mathcal{O}(\varepsilon^3)$ and $a_6^* = -u^{*2}/8 + \mathcal{O}(\varepsilon^3)$. It is generally expected that the fixed point is independent of the scale parameter s . In the exact renormalization, it is a consequence of the semigroup property. In the perturbation theory, it is expected to hold at each order of the expansion. The above considered fixed-point values obey this requirement within the given accuracy. It is obviously true also for the r^* value in the lowest order of the expansion, i. e.,

$$r^* = -\frac{c\Lambda^2}{2} \frac{n+2}{n+8} \varepsilon + \mathcal{O}(\varepsilon^2) . \quad (56)$$

However, it is less obvious for the next-order correction to r^* , as well as for other parameters of the fixed-point Hamiltonian. Therefore, we have performed some tests. Using (55), (19),

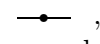
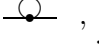
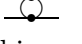
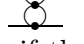
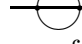
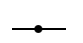

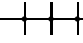
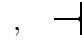
if the limit in (63) exists. In this case, rescaling the wave vectors by factor s/Λ , $\lim_{s \rightarrow \infty} \lim_{k \rightarrow 0} \{\cdot\}$ in (63) reduces to the expansion coefficient at $k^2 \ln s$ in the asymptotic large- s expansion of the diagram , in which $q \in [1, s]$ corresponds to the dotted lines. This coefficient can be calculated from (49) at $\zeta = s$, and is equal to $-K_4^2/4$. It yields the well known result (see, e. g., [2])

$$\eta = \frac{1}{2} \frac{n+2}{(n+8)^2} \varepsilon^2 + \mathcal{O}(\varepsilon^3) . \quad (64)$$

Closing this section, we note that the expected independence of the fixed-point function $\theta^*(\mathbf{k})$ on the RGT scale parameter s can be easily seen when using the diagrammatic representation (28): this diagram converges to certain s -independent value at $\zeta \rightarrow \infty$ (if the $\propto k^2$ contribution can be indeed subtracted), as discussed in Sec. 3.3.

4 Renormalization up to the order of ε^3

4.1 Vertices of the order $\mathcal{O}(\varepsilon^3)$

According to our diagrammatic representation, vertices of the order $\mathcal{O}(\varepsilon^3)$ in the renormalized Hamiltonian are those made by coupling three original vertices of (2), as well as other diagrams of such topology. Note that any diagram of the renormalized Hamiltonian containing a sub-graph (which is not the whole diagram) of topology , , , , , etc., i. e., a sub-graph with two outgoing lines, can be non-vanishing only if the lines of this sub-graph are the internal ones of the whole diagram. It is a consequence of two facts: 1) the sum of the wave vectors entering each node in a Feynman diagram is vanishing; 2) by definition of the RGT, the internal and the external lines in the diagrams of the renormalized Hamiltonian always have different values of $|\mathbf{k}|$. Thus, it is easy to verify that non-vanishing connected diagrams made of two vertices  and one vertex  can contain no more than two external lines. Moreover, the diagrams of order $\mathcal{O}(\varepsilon^3)$ with at least four external lines can have only the following topologies: , , and those ones obtained by coupling the lines in these graphs. In such a way, the renormalized Hamiltonian has the form

$$H = H^{(2)} + H^{(4)} + H^{(6)} + H^{(8)} + \mathcal{O}(\varepsilon^4) , \quad (65)$$

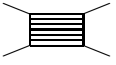
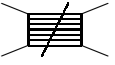

where $H^{(2m)}$ includes all the φ^{2m} -type vertices representable by the diagrams with $2m$ external lines. The corresponding algebraic representation is

$$\frac{H^{(2m)}}{T} = V^{1-m} \sum_{i_1, \dots, i_m} \sum_{\mathbf{k}_1, \mathbf{q}_1, \dots, \mathbf{k}_m, \mathbf{q}_m} Q_m(\mathbf{k}_1, \mathbf{q}_1, \dots, \mathbf{k}_m, \mathbf{q}_m) \varphi_{i_1, \mathbf{k}_1} \varphi_{i_1, \mathbf{q}_1} \cdots \varphi_{i_m, \mathbf{k}_m} \varphi_{i_m, \mathbf{q}_m} . \quad (66)$$

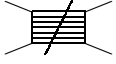
In such a form $Q_m(\mathbf{k}_1, \mathbf{q}_1, \dots, \mathbf{k}_m, \mathbf{q}_m)$ vanishes unless $\sum_i \mathbf{k}_i + \mathbf{q}_i = \mathbf{0}$. The dependence of these weight factors on various parameters is not indicated here.



As regards the quartic part $H^{(4)}$, we need to separate the contribution corresponding the ordinary φ^4 vertex, which is provided by the constant part of the weight function Q_2 in (66) evaluated at $\mathbf{k}_i = \mathbf{q}_i = \mathbf{0}$. For this purpose we can represent each diagram of $H^{(4)}$ as

$$\text{Diagram 1} = \text{Diagram 2} + \begin{pmatrix} \mathbf{0} \\ \text{Diagram 3} \\ \mathbf{0} \end{pmatrix} \times \text{Diagram 4} . \quad (67)$$

In this symbolic notation  is any diagram with four external lines, whereas  is the same diagram from which the contribution corresponding to the ordinary φ^4 vertex is subtracted. The latter one is represented by the last term in (67), where  is the diagram with amputated external lines having zero wave vectors. A particular example

$$\langle \text{---} \circ \text{---} \rangle = \langle \text{---} \text{---} \text{---} \rangle + \mathbf{0} \cdot \langle \text{---} \circ \text{---} \rangle \times \langle \text{---} \times \text{---} \rangle \quad (68)$$

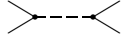
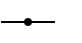
refers to the diagrams already considered in Sec. 3. A problem here is that not all diagrams of the kind  are convergent when the integration region for the internal lines $[\Lambda, \Lambda\zeta]$ is extended to infinity at $\zeta \rightarrow \infty$. To avoid possible unphysical divergence and instability of the RG flow, a suitable representation of the renormalized Hamiltonian should be used, where all vertices are convergent at $\zeta \rightarrow \infty$. It is reached by making appropriate zero- \mathbf{k} subtractions not

only from the entire φ^4 diagrams, but also from their internal parts, like, e. g.,  and . In the latter case, it is not necessary to make an extra subtraction of the zero- \mathbf{k} contribution from the whole diagram, since such a contribution is vanishing. Appropriate subtractions should be used also for vertices of higher than φ^4 order to ensure their convergence at $\zeta \rightarrow \infty$.

4.2 The renormalized Hamiltonian and RG flow equations

According to the analysis of Sec. 4, an appropriate representation of the renormalized Hamiltonian is

$$\begin{aligned} \frac{H}{T} &= \frac{1}{2} \sum_{i,\mathbf{k}} (r + ck^2 + \theta(\mathbf{k})) |\varphi_{i,\mathbf{k}}|^2 + \frac{u}{8} \langle \text{---} \text{---} \text{---} \rangle + a_4^{(1)} \Sigma \left(\langle \text{---} \text{---} \text{---} \rangle \right) \\ &+ a_4^{(2)} \Sigma \left(\langle \text{---} \text{---} \text{---} \rangle \right) + a_4^{(3)} \Sigma \left(\langle \text{---} \text{---} \text{---} \rangle \right) + a_4^{(4)} \Sigma \left(\langle \text{---} \text{---} \text{---} \rangle \right) \\ &+ a_6^{(1)} \Sigma \left(\langle \text{---} \text{---} \text{---} \rangle \right) + a_6^{(2)} \Sigma \left(\langle \text{---} \text{---} \text{---} \rangle \right) + a_6^{(3)} \Sigma \left(\langle \text{---} \text{---} \text{---} \rangle \right) \\ &+ a_6^{(4)} \Sigma \left(\langle \text{---} \text{---} \text{---} \rangle \right) + a_8 \Sigma \left(\langle \text{---} \text{---} \text{---} \rangle \right) + \mathcal{O}(\varepsilon^4), \end{aligned} \quad (69)$$

where $\Sigma(\cdot)$ denotes the sum of all such diagrams made of vertices  and , which yield the given picture when the dashed lines shrink to points. Besides, the combinatorial weight coefficients, including the n -dependent factors, are normalized in such a way that their sum is 1 at $n = 1$. The relations of the kind

$$\langle \text{---} \text{---} \text{---} \rangle = \mathbf{0} \cdot \langle \text{---} \text{---} \text{---} \rangle \times \langle \text{---} \text{---} \text{---} \rangle \quad (70)$$

$$\langle \text{---} \text{---} \text{---} \rangle = \mathbf{0} \cdot \langle \text{---} \text{---} \text{---} \rangle \times \langle \text{---} \text{---} \text{---} \rangle \quad (71)$$

have been applied to reduce the number of different kind of vertices in the representation of the Hamiltonian. The wave vectors of dotted lines are within $k \in [\Lambda, \Lambda\zeta]$ with ζ being updated as $\zeta' = s\zeta$ under the RG transformation R_s .

The other Hamiltonian parameters are updated as follows:

$$\begin{aligned}
u' &= s^{\varepsilon-2\eta} \left[u - \frac{n+8}{2} u^2 \mathbf{0} \text{---} \mathbf{0} + \frac{n^2+6n+20}{4} u^3 \left(\mathbf{0} \text{---} \mathbf{0} \right)^2 \right. \\
&+ (5n+22) u^3 \left(\mathbf{0} \text{---} \mathbf{0} + \mathbf{0} \text{---} \mathbf{0} + 2 \mathbf{0} \text{---} \mathbf{0} + 2 \mathbf{0} \text{---} \mathbf{0} + \mathbf{0} \text{---} \mathbf{0} \right) \\
&\left. + \frac{(n+2)(n+8)}{2} u^3 \left(\mathbf{0} \text{---} \mathbf{0} + \mathbf{0} \text{---} \mathbf{0} \right) + (n+8) u^2 r \mathbf{0} \text{---} \mathbf{0} \right] + \mathcal{O}(\varepsilon^4) \quad (72)
\end{aligned}$$

$$(a_4^{(1)})' = -\frac{9}{16} u^2 s^{2\varepsilon} \left(1 - (n+8) u \mathbf{0} \text{---} \mathbf{0} \right) + \mathcal{O}(\varepsilon^4) = -\frac{9}{16} u^2 + \mathcal{O}(\varepsilon^4) \quad (73)$$

$$(a_4^{(2)})' = \frac{27}{32} u^3 + \mathcal{O}(\varepsilon^4) \quad (74)$$

$$(a_4^{(3)})' = \frac{27}{8} u^3 + \mathcal{O}(\varepsilon^4) \quad (75)$$

$$(a_4^{(4)})' = \frac{9}{8} u^2 r' + \mathcal{O}(\varepsilon^4) \quad (76)$$

$$(a_6^{(1)})' = -\frac{1}{8} u^2 s^{2\varepsilon} \left(1 - (n+8) u \mathbf{0} \text{---} \mathbf{0} \right) + \mathcal{O}(\varepsilon^4) = -\frac{1}{8} u^2 + \mathcal{O}(\varepsilon^4) \quad (77)$$

$$(a_6^{(2)})' = \frac{9}{16} u^3 + \mathcal{O}(\varepsilon^4) \quad (78)$$

$$(a_6^{(3)})' = \frac{9}{8} u^3 + \mathcal{O}(\varepsilon^4) \quad (79)$$

$$(a_6^{(4)})' = \frac{1}{8} u^2 r' + \mathcal{O}(\varepsilon^4) \quad (80)$$

$$a_8' = \frac{3}{16} u^3 + \mathcal{O}(\varepsilon^4) . \quad (81)$$

Here $k \in [\Lambda/s, \Lambda]$ holds for solid lines, and $r' = s^2 \left(r + \frac{n+2}{2} u \mathbf{0} \text{---} \mathbf{0} \right) + \mathcal{O}(\varepsilon^2)$ is the updated value of r in the lowest order of the ε -expansion. We have skipped the refined RG flow equations for r , c , and $\theta(\mathbf{k})$, since those already considered in Sec. 3.1 are sufficient for our further analysis. These RG flow equations are proven by direct verification, as in Sec. 3.2.

The fixed-point values of the parameters $a_4^{(i)}$, $a_6^{(i)}$ and a_8 are trivially related to u^* and r^* . Namely, $(a_4^{(1)})^* = -(9/16)u^{*2} + o(\varepsilon^3)$, $(a_4^{(4)})^* = (9/8)u^{*2}r^* + o(\varepsilon^3)$, $(a_6^{(1)})^* = -(1/8)u^{*2} + o(\varepsilon^3)$, and similarly for other parameters. The value of u^* is

$$u^* = \frac{2c^2\Lambda^\varepsilon\varepsilon}{(n+8)K_d} \times \left(1 + a_1(n)\varepsilon + \mathcal{O}(\varepsilon^2) \right) . \quad (82)$$

The coefficient $a_1(n)$, calculated from (72), (56), and (64), is

$$a_1(n) = \frac{4(5n+22)}{K_4^2(n+8)^2} Q - \frac{n+2}{(n+8)^2} . \quad (83)$$

Here $Q = \hat{Q}(s)/\ln s$, where \hat{Q} is given by the diagram expression

$$\hat{Q}(s) = \left(\mathbf{0} \text{---} \mathbf{0} + \mathbf{0} \text{---} \mathbf{0} + 2 \mathbf{0} \text{---} \mathbf{0} + 2 \mathbf{0} \text{---} \mathbf{0} + \mathbf{0} \text{---} \mathbf{0} - \frac{1}{2} \left(\mathbf{0} \text{---} \mathbf{0} \right)^2 \right) \quad (84)$$

evaluated at $d = 4$ and $c = 1$. The quantity $\hat{Q}(s)$ is proportional to $\ln s$, since $\hat{Q}(s_1 s_2) = \hat{Q}(s_1) + \hat{Q}(s_2)$ holds at $\zeta \rightarrow \infty$ as a diagram identity, which can be verified by the method outlined in Sec. 3.4. Hence, Q is s -independent and, therefore, u^* is s -independent at least up to the ε^2 order, as expected. It is convenient to consider the limit $s \rightarrow \infty$ to determine Q from

$$\begin{aligned}
Q &= \lim_{s \rightarrow \infty} \left(\frac{\hat{Q}(s)}{\ln s} \right) = \lim_{s \rightarrow \infty} \left\{ \frac{1}{\ln s} \left[\text{diagram 1} - \frac{1}{2} \left(\text{diagram 2} \right)^2 \right] \right\} \\
&= \lim_{s \rightarrow \infty} \left\{ \frac{1}{\ln s} \left[\text{diagram 3} - \frac{1}{2} \left(\text{diagram 4} \right)^2 \right] \right\} = \lim_{s \rightarrow \infty} \left\{ \frac{1}{\ln s} \left[\text{diagram 5} + \frac{1}{2} \left(\text{diagram 6} \right)^2 \right] \right\} \\
&= \lim_{s \rightarrow \infty} \left\{ \frac{1}{\ln s} \left[K_4^2 \int_1^s \left(-\ln q + \frac{1}{2} \right) \frac{dq}{q} + \frac{1}{2} \left(K_4 \int_1^s \frac{dq}{q} \right)^2 \right] \right\} = \frac{K_4^2}{2}. \tag{85}
\end{aligned}$$

The wave vectors are rescaled to $k \in [1, s]$ (i. e., this interval corresponds to the dotted lines in the diagrams of (85)) and the zero- \mathbf{k} contribution of the internal diagram block is separated in the second line of (85). The large- k asymptotic estimate for diagram 5 , obtained in Sec. 3.3, is used in the third line of (85). Inserting this result into (83), we obtain

$$a_1(n) = \frac{3(3n + 14)}{(n + 8)^2}. \tag{86}$$

Summarising the results of this section, one has to note that, at the ε^3 order, the renormalized Hamiltonian contains several extra vertices as compared to the initial or bare Hamiltonian. All these terms, including the φ^6 vertices and the φ^8 vertex, are relevant in the sense that they do not vanish at the fixed point. Moreover, they are always relevant in the same sense as the φ^4 vertex, because of the relations between $a_6^{(i)}$, a_8 and u . In particular, if we consider the RG flow starting slightly away from the critical surface, then those terms are considered as relevant, which diverge at large renormalization scales $\zeta \rightarrow \infty$. The shrinking terms are irrelevant in this usual sense. The φ^4 vertex is commonly considered as relevant in $4 - \varepsilon$ dimensions. Consequently, the φ^6 and φ^8 vertices are also relevant in the same (usual) sense.

5 Expansion at a fixed spatial dimension d

Apart from the ε -expansion, we have tested also an alternative approach, where the coupling constant u is considered as an expansion parameter at a fixed spatial dimensionality, i. e., fixed ε . In this sense the discussed here approach is similar in spirit to that widely used for calculations in three dimensions, $d = 3$, as described in [14, 15, 16, 17, 18]. This known approach uses the Callan-Symanzik equation instead of the Wilson's equation (3). However, if both are correct RG equations, then they should provide consistent results. Here we use (3) to make the expansion in powers of u at a fixed but small ε .

In this method, all the rescaling factors of the kind s^ε have to be retained in their original form without the expansion in powers of ε . Following the approach of [14, 15, 16, 17, 18], the critical exponents should be expanded in powers of the coupling constant, estimating their universal values at $u = u^*$. Therefore, the correction factors like $s^{-\eta}$ can be omitted in the first approximation, since one finds that $\eta = \mathcal{O}(u^2)$. Using this idea, and following the calculations

after the RG transformation R_s , transforming the original Hamiltonian H into the renormalized one $R_s H$. It is a general exact relation, trivially following from the fact that the integration over the Fourier modes with $\Lambda/s < k < \Lambda$ in the first step of the RG transformation does not alter the correlation function for $k < \Lambda/s$, whereas the s -dependent factors in (91) compensate its rescaling in the second step of the RG transformation (see Sec. 2).

6.2 The two-point correlation function at the fixed point

In the following, we will examine the two-point correlation function (or its inverse) at the fixed point up to the ε^2 order. According to (91), $X(\mathbf{k}) = ak^{2-\eta}$ holds within $k \leq \Lambda$ for the fixed-point Hamiltonian H^* (since $R_s H^* = H^*$) with some \mathbf{k} -independent constant a , which can depend on n , ε , and Hamiltonian parameters. It is consistent with (90) if

$$ak^2(1 - \eta \ln k) = ck^2 - \frac{n+2}{2}u^{*2} \left\{ \text{diagram 1} + \text{diagram 2} + 3 \left(\text{diagram 3} + \text{diagram 4} \right) \right\} + \mathcal{O}(\varepsilon^3) \quad (92)$$

holds for $k \leq \Lambda$, since $\tilde{\Sigma}(\mathbf{0})$ vanishes at the fixed point. Note that $q \in [0, \Lambda]$ refers to the solid lines and $q \in [\Lambda, \Lambda\zeta]$ at $\zeta \rightarrow \infty$ – to the dotted lines in (92). The diagrams can be evaluated at $d = 4$ in this case, and we can set $c = 1$, as it gives merely a common factor. By definition of

diagram 1 , we have

$$\text{diagram 1} = \text{diagram 2} - k^2 R(\zeta), \quad (93)$$

where

$$R(\zeta) = \lim_{k \rightarrow 0} \left\{ \frac{1}{k^2} \text{diagram 2} \right\} = -\frac{K_4^2}{4} \ln \zeta + \text{const} \quad \text{at } d = 4, \quad \zeta \rightarrow \infty, \quad (94)$$

as consistent with the already considered estimation of such term (after rescaling the wave vectors from $q \in [\Lambda, \Lambda\zeta]$ to $q \in [1, \zeta]$) at the end of Sec. 3.5, provided that the considered here limit (at $k \rightarrow 0$) exists. As in Sec. 3.5, this ensures the expected properties. Inserting (93) into (92), and summing up the diagrams, we obtain (at $c = 1$)

$$ak^2(1 - \eta \ln k) = k^2 - \frac{n+2}{2}u^{*2}f(k, \zeta) + \mathcal{O}(\varepsilon^3) \quad \text{at } \zeta \rightarrow \infty, \quad (95)$$

where

$$f(k, \zeta) = \text{diagram 3} - k^2 R(\zeta) \quad (96)$$

with $q \in [0, \Lambda\zeta]$ corresponding to the dashed lines. Using (94) and rescaling the wave vectors, we find that

$$f(k) = \lim_{\zeta \rightarrow \infty} f(k, \zeta) \quad (97)$$

obeys the equation

$$f(sk) = s^2 \left(f(k) + \frac{1}{4}K_4^2 k^2 \ln s \right) \quad (98)$$

with the solution

$$f(k) = \mathcal{B}k^2 + \frac{1}{4}K_4^2 k^2 \ln k, \quad (99)$$

where \mathcal{B} is a constant. According to this, Eq. (95) is indeed satisfied with appropriate $a = a(n, \varepsilon)$ at η given by (64). Thus, the ε -expansion of $X(\mathbf{k})$ at the fixed point is consistent with the scaling $X(\mathbf{k}) = ak^{2-\eta}$ within $k \leq \Lambda$ up to the order of ε^2 , at least, if the limit (94) exists. Besides, such analysis provides one more method to determine the critical exponent η .

can be expanded in powers of k at $d < 4$ for large renormalization scales $s \rightarrow \infty$. According to (91), it is true for the bare Hamiltonian at $k \rightarrow 0$. Eq. (91) then yields

$$X(\mathbf{k}; R_s^m H_0) = A(\delta_0, \varepsilon) k^{2-\eta} \left\{ 1 + \sum_i a_i(\delta_0, \varepsilon) s^{-m\omega_i} k^{\omega_i} + \sum_i \hat{a}_i(\delta_0, \varepsilon) s^{-m\hat{\omega}_i} k^{\hat{\omega}_i} \right\} \quad \text{at } k \rightarrow 0, \quad (104)$$

where $R_s^m H_0$ denotes the renormalized Hamiltonian after m RG transformations R_s . The well known result of the ε -expansion states that the leading correction-to-scaling exponent is

$$\omega := \omega_1 = \varepsilon + \mathcal{O}(\varepsilon^2). \quad (105)$$

In the following, we will formulate as a theorem an important result, stating certain consistency relations for the coefficients and exponents in (103).

Theorem. *If the perturbative ε -expansion-based renormalization (repeating the RG transformation R_s) of $X(\mathbf{k}) = 1/G(\mathbf{k})$ on the critical surface is consistent with (103) and (104) at any small ε -independent δ_0 and δ , such that $0 < \delta/\delta_0 < 1$, defining the initial (δ_0) and the final (δ) value of $(u - u^*)/u^*$ (with u^* determined at the current c), then*

$$\omega_j = j\varepsilon + \mathcal{O}(\varepsilon^2) \quad : \quad j \geq 1, \quad (106)$$

$$A(\delta_0, \varepsilon) = c_0 + \mathcal{O}(\varepsilon), \quad (107)$$

$$a_j(\delta_0, \varepsilon) = b_j \varepsilon \left(\frac{\delta_0}{1 + \delta_0} \right)^j + \mathcal{O}(\varepsilon^2) \quad : \quad j \geq 1 \quad (108)$$

hold, where c_0 is the initial value of c , and $b_j = -\eta_2(j+1)/j$, where η_2 is defined in $\eta = \eta_2 \varepsilon^2 + \mathcal{O}(\varepsilon^3)$.

Proof. Let us first determine the number $m = m(\delta_0, \delta, s, \varepsilon)$ of RGT required for transformation of $(u - u^*)/u^*$ from δ_0 to δ . From (21) we obtain the updating rule for $\delta_\ell = (u_\ell - u_\ell^*)/u_\ell^*$,

$$\frac{\delta_{\ell+1}}{\delta_\ell} = s^{-\varepsilon(1+\delta_\ell) + \mathcal{O}(\varepsilon^2)}, \quad (109)$$

where u_ℓ is the value of u after ℓ -th RGT, and $u_\ell^* = u^*(c_\ell)$ is the fixed-point value of u determined at the current c after ℓ -th RGT, i. e., at $c = c_\ell$. Here we take into account that $c_{\ell+1} = c_\ell + \mathcal{O}(\varepsilon^2)$ holds according to (23) and therefore $u_{\ell+1}^* = u_\ell^* + \mathcal{O}(\varepsilon^3)$ follows from (82). Denoting $x_\ell = \ln |\delta_\ell|$, Eq. (109) reduces to

$$x_{\ell+1} - x_\ell = -\varepsilon (1 + \text{sign}(\delta) e^{x_\ell}) \ln s + \mathcal{O}(\varepsilon^2). \quad (110)$$

The variation of x_ℓ becomes quasi-continuous in the limit $\varepsilon \rightarrow 0$, so that x_ℓ can be considered as a continuous function $x(\ell)$, and (110) transforms into the differential equation

$$\frac{dx(\ell)}{d\ell} = -\varepsilon (1 + \text{sign}(\delta) e^x) \ln s + \mathcal{O}(\varepsilon^2). \quad (111)$$

Integrating this equation, we find the necessary number of RGT

$$m = \frac{1}{\varepsilon \ln s} \int_{x_*}^{x_0} \frac{dx}{1 + \text{sign}(\delta) e^x} + \mathcal{O}(1) = \frac{1}{\varepsilon \ln s} \ln \left[\frac{\delta_0(1 + \delta)}{(1 + \delta_0)\delta} \right] + \mathcal{O}(1), \quad (112)$$

where $x_0 = \ln |\delta_0|$ is the initial and $x_* = \ln |\delta|$ is the final value of $\ln |\delta_\ell|$. It yields

$$s^{-m\varepsilon} = \frac{1 + \delta_0}{\delta_0} \times \frac{\delta}{1 + \delta} + \mathcal{O}(\varepsilon). \quad (113)$$

Inserting (113) into (104), we obtain

$$X(\mathbf{k}; R_{s^m} H_0) = A(\delta_0, \varepsilon) k^{2-\eta} \left\{ 1 + \sum_i a_i(\delta_0, \varepsilon) \left[\frac{\delta(1 + \delta_0)}{(1 + \delta)\delta_0} + \mathcal{O}(\varepsilon) \right]^{\omega_i/\varepsilon} k^{\omega_i} + \mathcal{O}\left(e^{-\lambda/\varepsilon} k^{\hat{\omega}}\right) \right\}, \quad (114)$$

where the terms with $\hat{\omega}_i$ are absorbed in the last remainder term, where $\lambda > 0$ and $\hat{\omega}$ is the smallest exponent among $\hat{\omega}_i$. This term is irrelevant in the ε -expansion.

From (102) we obtain

$$X(\mathbf{k}; R_{s^m} H_0) = ck^2 - \frac{n+2}{2c^3} [u^*(1 + \delta)]^2 \left(\mathcal{B} k^2 + \frac{1}{4} K_4^2 k^2 \ln k \right) + \mathcal{O}(\varepsilon^3). \quad (115)$$

The diagrams of (102) are evaluated in (115) as in Sec. 6.2 (cf. Eq. (99)), since the difference between the cases $\zeta = \infty$ and $\zeta = s^{m(\delta_0, \delta, s, \varepsilon)}$ (with $q \in [\Lambda, \Lambda\zeta]$ for dotted lines) is irrelevant within the ε -expansion. Since c is renormalized by $\mathcal{O}(\varepsilon^2)$ in one RGT according to (23), the renormalized c value after $m \sim 1/\varepsilon$ RG transformations in (115) is $c = c_0 + \mathcal{O}(\varepsilon)$.

The consistency with (114) (where $\omega_i \rightarrow 0$ at $\varepsilon \rightarrow 0$) implies that $X(\mathbf{k}; R_{s^m} H_0)$ can be expanded as

$$X(\mathbf{k}; R_{s^m} H_0) = k^2 \left(\mathcal{B}_0(\delta_0, \delta, \varepsilon) + \mathcal{B}_1(\delta_0, \delta, \varepsilon) \ln k + \mathcal{B}_2(\delta_0, \delta, \varepsilon) (\ln k)^2 + \dots \right) \quad (116)$$

at $\varepsilon \rightarrow 0$. On the other hand, the diagrammatic perturbative equation for $X(\mathbf{k}; R_{s^m} H_0)$ on the critical surface can be represented in general (up to any order of the ε -expansion) as

$$X(\mathbf{k}; R_{s^m} H_0) = c F(\mathbf{k}, \delta, \varepsilon), \quad (117)$$

where $c = c(\delta_0, \delta, \varepsilon)$, whereas $F(\mathbf{k}, \delta, \varepsilon)$ contains only integer powers of δ in the small- δ -expansion. It is because the critical value of r , as well as all Hamiltonian parameters can be expanded in integer powers of $u = u^*(1 + \delta)$, where $u^* = u^*(c) = c^2 u^*(1)$ holds with δ_0 - and δ -independent $u^*(1)$, and the diagrams associated with u^ℓ contain $2\ell - 1$ internal coupling lines giving the factor $c^{1-2\ell}$. These are consequences of the general structure of the RG flow equations. Hence, the small- δ -expansion of the ratio $\mathcal{B}_i(\delta_0, \delta, \varepsilon)/\mathcal{B}_0(\delta_0, \delta, \varepsilon)$ in (116) contains only integer powers of δ for any $i \geq 1$. Assuming that $\omega_j = d_j \varepsilon + \mathcal{O}(\varepsilon^2)$ holds with non-integer positive d_j for some j , we arrive at a contradiction, since then the ε -expansion in (114) produces $\mathcal{B}_i(\delta_0, \delta, \varepsilon)/\mathcal{B}_0(\delta_0, \delta, \varepsilon)$ containing non-integer powers of δ . The contradiction is obtained also if we assume the existence of ω_j of a higher order than $\mathcal{O}(\varepsilon)$, since the ε -expansion of $\mathcal{B}_i(\delta_0, \delta, \varepsilon)/\mathcal{B}_0(\delta_0, \delta, \varepsilon)$ in (114) produces powers of $\ln \delta$ in this case. We can consider also a possibility that $\omega_j \sim \varepsilon^{\mu_j}$ with non-integer μ_j holds for some indices j . It does not lead to the consistency, since the expansion of $F(\mathbf{k}, \delta, \varepsilon)$ contains only integer powers of ε , coming from the ε -expansion of u^* and diagrams evaluated at $c = 1$. In such away, (114) can be consistent with the diagrammatic perturbative equation only if (105) and (106) hold.

$X(\mathbf{k}; R_{s^m} H_0) = ck^2 + \mathcal{O}(\varepsilon^2) = c_0 k^2 + \mathcal{O}(\varepsilon)$ holds according to (115). Besides, the coefficient at $\ln k$ in (115) is of order $\mathcal{O}(\varepsilon^2)$, and it is independent of δ_0 at this order. Eqs. (107) and (108)

must hold to satisfy these relations in (114), performing the ε -expansion. Finally, the equation

$$-\eta + \varepsilon^2 \sum_{j \geq 1} j b_j \left(\frac{\delta}{1 + \delta} \right)^j = -\eta(1 + \delta)^2 + \mathcal{O}(\varepsilon^3) , \quad (118)$$

states the necessary consistency relation for the coefficient at $\varepsilon^2 \ln k$ in (114) and (115), taking into account that $[(n+2)/(8c^3)]K_4^2 u^{*2} = c\eta + \mathcal{O}(\varepsilon^3)$ holds according to (55) and (64). From (118) we find $b_j = -\eta_2(j+1)/j$, taking into account that $\sum_{j=1}^{\infty} (j+1)x^j = \frac{\partial}{\partial x} \sum_{j=1}^{\infty} x^{j+1} = (2x - x^2)/(1-x)^2$ and setting here $x = \delta/(1+\delta)$. \square

6.4 A test of consistency for the correlation function

6.4.1 A diagrammatic consistency relation

Based on the relations stated in the above theorem, here we perform some test for single RG transformation R_s on the critical surface, starting with small $(u - u^*)/u^* = \delta_0$, defined as before.

We consider the asymptotic small- \mathbf{k} estimate of the inverse correlation function defined as

$$X^{as}(\mathbf{k}; H_0) := A(\delta_0, \varepsilon) k^{2-\eta} \left\{ 1 + \sum_i a_i(\delta_0, \varepsilon) k^{\omega_i} \right\} \quad (119)$$

obtained by neglecting the irrelevant (at $k \rightarrow 0$) terms with exponents $\hat{\omega}_i$ in (103). Following (91), it rescales exactly as

$$X^{as}(\mathbf{k}; R_s H_0) = A(\delta_0, \varepsilon) k^{2-\eta} \left\{ 1 + \sum_i a_i(\delta_0, \varepsilon) s^{-\omega_i} k^{\omega_i} \right\} \quad (120)$$

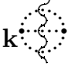
after the RG transformation R_s . According to (108), we can write

$$a_i(\delta_0, \varepsilon) = b_i \varepsilon \left(\frac{\delta_0}{1 + \delta_0} \right)^i + \mathcal{E}_i(\delta_0) \varepsilon^2 + \mathcal{O}(\varepsilon^3) \quad : \quad i \geq 1 , \quad (121)$$

where $\mathcal{E}_i(\delta_0)$ are some unknown coefficients. Further on, we consider the expansion up to the ε^2 order for the ratio $X^{as}(\mathbf{k}; R_s H_0)/X^{as}(\mathbf{k}; H_0)$, in which case these unknown terms cancel, i. e.,

$$\frac{X^{as}(\mathbf{k}; R_s H_0)}{X^{as}(\mathbf{k}; H_0)} = 1 - \varepsilon^2 \ln s \sum_i i b_i \left(\frac{\delta_0}{1 + \delta_0} \right)^i + \mathcal{O}(\varepsilon^3) = 1 + \eta \ln s \left[(1 + \delta_0)^2 - 1 \right] + \mathcal{O}(\varepsilon^3) . \quad (122)$$

In the following, we calculate the ratio $X^{as}(\mathbf{k}; R_s H_0)/X^{as}(\mathbf{k}; H_0)$ from the diagram equation (102) and compare the results. In this case we need to include those terms, which correspond to $X^{as}(\mathbf{k}; R_s H_0)$ and $X^{as}(\mathbf{k}; H_0)$ in the ε -expansion. Thus, the terms containing $k^2(\ln k)^\ell$ with $\ell \geq 0$ must be included, whereas those containing $k^\mu(\ln k)^\ell$ with $\mu > 2$ have to be neglected. Any quantity endowed with superscript “*as*” is calculated in this way. Furthermore, both $X^{as}(\mathbf{k}; R_s H_0)$ and $X^{as}(\mathbf{k}; H_0)$ are proportional to the initial c value c_0 , so that we can calculate their ratio at $c_0 = 1$ without loss of generality. According to the assumption of the existence of limit $\lim_{k \rightarrow 0} \left\{ \frac{1}{k^2} (\cdot) \right\}$ for the diagrams entering the RG flow equation for c , the term $\theta(\mathbf{k})$, repre-

sented by , tends to zero faster than $\sim k^2$ at $k \rightarrow 0$. Therefore, it is neglected. Thus, the diagram equation at $c_0 = 1$ yields

$$X^{as}(\mathbf{k}; H_0) = k^2 - \frac{n+2}{2} u^{*2} (1 + \delta_0)^2 \left(\text{diagram: circle with slash, solid left, dotted right} \right)^{as} + \mathcal{O}(\varepsilon^3) \quad (123)$$

$$\begin{aligned} X^{as}(\mathbf{k}; R_s H_0) &= ck^2 - \frac{n+2}{2} u^{*2} (1 + \delta_0)^2 \left[\left(\text{diagram: circle with slash, solid left, dotted right} \right)^{as} + \right. \\ &\quad \left. 3 \left\{ \left(\text{diagram: circle with slash, solid left, dotted right} \right)^{as} + \left(\text{diagram: circle with slash, dotted left, solid right} \right)^{as} \right\} \right] + \mathcal{O}(\varepsilon^3), \end{aligned} \quad (124)$$

where $q \in [0, \Lambda]$ holds for the solid lines and $q \in [\Lambda, \Lambda s]$ – for the dotted lines. Here we have set $u = u^*(1 + \delta_0)$ in both expressions, since u^2 after the RGT is varied only by $\mathcal{O}(\varepsilon^3)$. The quantity $\left(\text{diagram: circle with slash, solid left, dotted right} \right)^{as}$ cancels in $X^{as}(\mathbf{k}; R_s H_0)/X^{as}(\mathbf{k}; H_0)$, calculated up to the ε^2 order. The renormalized c in (124), calculated from (23), is

$$c = 1 - \eta \ln s - \frac{n+2}{2} u^{*2} (1 + \delta_0)^2 \lim_{k \rightarrow 0} \left\{ \frac{1}{k^2} \left(\text{diagram: circle with slash, solid left, dotted right} \right) \right\} \Big|_{d=4} + \mathcal{O}(\varepsilon^3) \quad (125)$$

with $q \in [\Lambda/s, \Lambda]$ corresponding to the solid lines in the diagram evaluated at $c = 1$. If this diagram is completed by $3 \left(\text{diagram: circle with slash, solid left, dotted right} + \text{diagram: circle with slash, dotted left, solid right} \right)$ with $q \in [\Lambda/s, \Lambda]$ for the solid lines and $q \in [\Lambda, \infty]$ for the dotted lines, then the obtained expression $\lim_{k \rightarrow 0} \left\{ \frac{1}{k^2} (\cdot) \right\} \Big|_{d=4}$ is exactly $\propto \ln s$, as it follows from the diagram identity (62) provided that this limit, as well as the limit in (125), exists. Recall that we test the scenario when this expected property holds. The proportionality coefficient is $-K_4^2/4$, in accordance with the calculations at $s \rightarrow \infty$ in Sec. 3.5. Setting further $\Lambda = 1$ for simplicity, we can write

$$\lim_{k \rightarrow 0} \left\{ \frac{1}{k^2} \left(\text{diagram: circle with slash, solid left, dotted right} \right) \right\} \Big|_{d=4} = -\frac{K_4^2}{4} \ln s - 3 \lim_{k \rightarrow 0} \frac{D(1/s, \infty; \mathbf{k})}{k^2}, \quad (126)$$

where

$$D(\Lambda_1, \Lambda_2; \mathbf{k}) := \text{diagram: circle with slash, solid left, dotted right} + \text{diagram: circle with slash, dotted left, solid right} \quad (127)$$

with $q \in [\Lambda_1, 1]$ for the solid lines and $q \in [1, \Lambda_2]$ for the dotted lines.

Summarizing all the derived here diagrammatic relations for $X^{as}(\mathbf{k}; R_s H_0)$ and $X^{as}(\mathbf{k}; H_0)$, and also $[(n+2)/(8c^3)]K_4^2 u^{*2} = c\eta + \mathcal{O}(\varepsilon^3)$, we finally obtain

$$\frac{X^{as}(\mathbf{k}; R_s H_0)}{X^{as}(\mathbf{k}; H_0)} = 1 + \eta \left\{ [(1 + \delta_0)^2 - 1] \ln s - \frac{12}{K_4^2} (1 + \delta_0)^2 \frac{D(0, s; \mathbf{k}) - D(1/s, \infty; \mathbf{k})}{k^2} \right\} + \mathcal{O}(\varepsilon^3) \quad (128)$$

at $k \rightarrow 0$. It is evident that (122) and (128) agree with each other if and only if

$$D^{as}(0, s; \mathbf{k}) = D^{as}(1/s, \infty; \mathbf{k}) \quad \text{at } d = 4, \quad (129)$$

holds for $s > 1$, at the condition that the limits in (126) exist, as expected.

6.4.2 Scaling relation

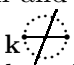
Here we consider the exact scaling relation

$$s^{2-2\varepsilon} [D(0, \infty; \mathbf{k}/s) - D(1/s, \infty; \mathbf{k}/s)] = [D(0, \infty; \mathbf{k}) - D(0, s; \mathbf{k})]. \quad (130)$$

It is proven as follows. Considering $D(0, \infty; \mathbf{k}/s) - D(1/s, \infty; \mathbf{k}/s)$, we decompose the $q \in [0, 1]$ lines of the diagrams of $D(0, \infty; \mathbf{k}/s)$ in two lines with $q \in [0, 1/s]$ and $q \in [1/s, 1]$. Similarly, for $D(0, \infty; \mathbf{k}) - D(0, s; \mathbf{k})$, we decompose the $q \in [1, \infty]$ lines of the diagrams of $D(0, \infty; \mathbf{k})$ in $q \in [1, s]$ and $q \in [s, \infty]$. Then, it is easy to see that $D(0, \infty; \mathbf{k}/s) - D(1/s, \infty; \mathbf{k}/s)$ is represented by the sum of all such diagrams with three kind of lines, having wave vectors within $[0, 1/s]$, $[1/s, 1]$ and $[1, \infty]$, respectively, which contain at least one line within $[0, 1/s]$ and at least one line within $[1, \infty]$. Similarly, $D(0, \infty; \mathbf{k}) - D(0, s; \mathbf{k})$ is represented by the sum of all such diagrams with three kind of lines, having wave vectors within $[0, 1]$, $[1, s]$ and $[s, \infty]$, respectively, which contain at least one line within $[0, 1]$ and at least one line within $[s, \infty]$. Rescaling the wave vectors in the diagrams of $D(0, \infty; \mathbf{k}/s) - D(1/s, \infty; \mathbf{k}/s)$ by factor s and multiplying the result with $s^{2-2\varepsilon}$, we obtain just the diagrams of $D(0, \infty; \mathbf{k}) - D(0, s; \mathbf{k})$. It proves (130).

According to (130), the condition (129) is satisfied if $D(0, \infty; \mathbf{k}) - D(1/s, \infty; \mathbf{k}) \propto k^2$ holds at $k \rightarrow 0$ in four dimensions. However, allowing a possibility that $D(0, \infty; \mathbf{k})/k^2$ diverges at $k \rightarrow 0$, this condition might be not satisfied.

6.4.3 Evaluation of $D(1/s, \infty; \mathbf{k})$ in four dimensions

In the following we consider the case $s = 1 + ds$, where ds is small and positive, and evaluate the diagrams of $D(1/s, \infty; \mathbf{k})$ at $d = 4$. In particular, the diagram , having wave vectors within $[1/s, 1]$ for the solid line and $[1, \infty]$ for the dotted lines, can be calculated as follows:

$$\mathbf{k} \begin{array}{c} \text{---} \\ \text{---} \\ \text{---} \end{array} = \frac{2K_4}{\pi} \int_{1/s}^1 q dq \int_0^\pi [J(|\mathbf{q} + \mathbf{k}|) - J(q)] \sin^2 \theta d\theta, \quad (131)$$

where θ is the angle made by vectors \mathbf{q} and \mathbf{k} (i. e., $|\mathbf{q} + \mathbf{k}|^2 = q^2 + 2kq \cos \theta + k^2$) and

$$\begin{aligned} J(q) &= \mathbf{q} \begin{array}{c} \text{---} \\ \text{---} \\ \text{---} \end{array} = \frac{2K_4}{\pi} \int_1^{1+q} k dk \int_0^{\hat{\theta}(q,k)} \frac{\sin^2 \theta d\theta}{q^2 + 2kq \cos \theta + k^2} - K_4 \ln(1+q) \\ &+ \frac{2K_4}{\pi} \int_{1+q}^\infty k dk \int_0^\pi \left(\frac{1}{q^2 + 2kq \cos \theta + k^2} - \frac{1}{k^2} \right) \sin^2 \theta d\theta \quad \text{for } 0 < q < 2, \end{aligned} \quad (132)$$

where

$$\hat{\theta}(q, k) = \arccos \left(\frac{1 - q^2 - k^2}{2kq} \right). \quad (133)$$

Using the small- \mathbf{k} expansion

$$J(|\mathbf{q} + \mathbf{k}|) = J(q) + \frac{dJ}{dq} \left(k \cos \theta + \frac{k^2}{2q} \sin^2 \theta \right) + \frac{1}{2} \frac{d^2 J}{dq^2} k^2 \cos^2 \theta + \mathcal{O}(k^3), \quad (134)$$

we obtain

$$\left(\mathbf{k} \begin{array}{c} \text{---} \\ \text{---} \\ \text{---} \end{array} \right)^{as} = k^2 \times \frac{K_4}{8} \int_{1/s}^1 (3J'(q) + qJ''(q)) dq . \quad (135)$$

This method is certainly valid for small ds , since in this case $J(q)$ is an analytic function of q within the whole integration region, i. e., around $q = 1$.

The diagram $\mathbf{k} \begin{array}{c} \text{---} \\ \text{---} \\ \text{---} \end{array}$ is calculated similarly:

$$\left(\mathbf{k} \begin{array}{c} \text{---} \\ \text{---} \\ \text{---} \end{array} \right)^{as} = k^2 \times \frac{K_4}{8} \int_{1/s}^1 (3\tilde{J}'(q) + q\tilde{J}''(q)) dq , \quad (136)$$

where

$$\tilde{J}(q) = \mathbf{q} \begin{array}{c} \text{---} \\ \text{---} \\ \text{---} \end{array} = \frac{2K_4}{\pi} \int_{1/s}^1 k dk \int_0^{\hat{\theta}(q,k)} \frac{\sin^2 \theta d\theta}{q^2 + 2kq \cos \theta + k^2} . \quad (137)$$

Again, this method is valid for small ds , since $\tilde{J}(q)$ is an analytic function of q around $q = 1$. Summing up (135) and (136) and expanding in a Taylor series of ds at $ds \rightarrow 0$, we obtain

$$\begin{aligned} D^{as}(1/s, \infty; \mathbf{k}) &= k^2 \times \frac{K_4}{8} \left\{ (3J'(1) + J''(1)) ds + \lim_{ds \rightarrow 0} \left(\frac{3\tilde{J}'(1) + \tilde{J}''(1)}{ds} \right) \times (ds)^2 \right. \\ &\quad \left. - \left(3J'(1) + 3J''(1) + \frac{1}{2}J'''(1) \right) (ds)^2 + \mathcal{O}((ds)^3) \right\} . \end{aligned} \quad (138)$$

We have evaluated $J(q)$, $\tilde{J}(q)$ and their derivatives at $q = 1$: $J(1) \simeq -0.214068K_4$, $J'(1) \simeq -0.217996K_4$, $J''(1) \simeq -0.012680K_4$, $J'''(1) \simeq -0.0177K_4$, $\lim_{ds \rightarrow 0} (\tilde{J}'(1)/ds) = \left(\frac{\sqrt{3}}{\pi} - \frac{2}{3} \right) K_4$ and $\lim_{ds \rightarrow 0} (\tilde{J}''(1)/ds) \simeq -0.021539K_4$. Most of these values have been obtained calculating numerically the corresponding integrals. These values satisfy certain expected relation, given in the next subsection, and, thus, must be correct within the given numerical accuracy.

6.4.4 Consistency relation for $D^{as}(0, s; \mathbf{k})$

According to calculations in the previous subsection, $D(1/s, \infty; \mathbf{k})$ at small ds is asymptotically proportional to k^2 at $k \rightarrow 0$ with non-zero proportionality coefficient. Based on this fact, and using diagram identities, here we derive a necessary consistency relation for $D^{as}(0, s; \mathbf{k})$ at which (129) can hold. As in previous section, here any diagram relation refers to the case $d = 4$.

Let us introduce the notation

$$Q(\Lambda; \mathbf{k}) := \mathbf{k} \begin{array}{c} \text{---} \\ \text{---} \\ \text{---} \end{array} , \quad (139)$$

where the wave vectors of the coupling lines are within $[0, \Lambda]$. In the following, we use the relation

$$f(k) = \mathbf{k} \begin{array}{c} \text{---} \\ \text{---} \\ \text{---} \end{array} + 3 \left(\mathbf{k} \begin{array}{c} \text{---} \\ \text{---} \\ \text{---} \end{array} + \mathbf{k} \begin{array}{c} \text{---} \\ \text{---} \\ \text{---} \end{array} \right) \equiv Q(1; \mathbf{k}) + 3D(0, \infty; \mathbf{k}) = \mathcal{B} k^2 + \frac{1}{4} K_4^2 k^2 \ln k \quad \text{at } k \rightarrow 0 , \quad (140)$$

which follows from the equations of Sec. 6.2, taking into account that $\mathbf{k} \circledast$ decays faster than k^2 at $k \rightarrow 0$ (according to the assumed expected properties – see Sec. 3.1). Note that the wave vectors of the solid lines are within $[0, 1]$ and those of the dotted lines are within $[1, \infty]$ in (140).

Since $D(1/s, \infty; \mathbf{k}) \propto k^2$ holds at $k \rightarrow 0$, we have $s^2 D(1/s, \infty; \mathbf{k}/s) = D(1/s, \infty; \mathbf{k})$ in this limit. Assuming that (129) holds, we have $D(0, s; \mathbf{k}) = D(1/s, \infty; \mathbf{k})$ at $k \rightarrow 0$. Inserting these relations into (130) at $\varepsilon = 0$, we obtain the asymptotic relation $s^2 D(0, \infty; \mathbf{k}/s) = D(0, \infty; \mathbf{k})$ for small k , which means that $D(0, \infty; \mathbf{k}) \propto k^2$ holds at $k \rightarrow 0$. According to the latter, Eq. (140) gives us

$$Q(1; \mathbf{k}) = \mathcal{B}_1 k^2 + \frac{1}{4} K_4^2 k^2 \ln k \quad \text{at } k \rightarrow 0, \quad (141)$$

where \mathcal{B}_1 is some constant. Using (141) and the scaling relation

$$Q(s; \mathbf{k}) = s^2 Q(1; \mathbf{k}/s), \quad (142)$$

we obtain

$$Q(1 + ds; \mathbf{k}) - Q(1; \mathbf{k}) = -\frac{1}{4} K_4^2 \left(ds - \frac{1}{2} (ds)^2 + \mathcal{O}((ds)^3) \right) \times k^2 \quad \text{at } k \rightarrow 0. \quad (143)$$

Consider now the diagram identity

$$\mathbf{k} \circledast + 3 \left(\mathbf{k} \circledast + \mathbf{k} \circledast \right) = \mathbf{k} \circledast - \mathbf{k} \circledast, \quad (144)$$

where $[0, 1]$ corresponds to the solid lines, $[1, 1 + ds]$ – to the dotted lines and $[0, 1 + ds]$ – to the dashed lines. The last diagram in (144) can be evaluated by the method used in Sec. 6.4.3, leading to the conclusion that it is $\propto k^2 (ds)^3$ at $k \rightarrow 0$ and small ds . Hence, according to the definitions (139) and (127), the identity (144) yields

$$3D(0, 1 + ds; \mathbf{k}) = Q(1 + ds; \mathbf{k}) - Q(1; \mathbf{k}) + \mathcal{O}(k^2 (ds)^3). \quad (145)$$

Inserting here (143), we obtain

$$D^{as}(0, 1 + ds; \mathbf{k}) = \frac{1}{12} K_4^2 \left(-ds + \frac{1}{2} (ds)^2 + \mathcal{O}((ds)^3) \right) \times k^2 \quad (146)$$

at small ds . This relation has been derived assuming (129). Thus, this is a necessary condition at which (129) can hold. According to (129) and (146), we must have also

$$D^{as}(1/s, \infty; \mathbf{k}) = \frac{1}{12} K_4^2 \left(-ds + \frac{1}{2} (ds)^2 + \mathcal{O}((ds)^3) \right) \times k^2 \quad (147)$$

for $s = 1 + ds$. The latter relation is really satisfied in accordance with the numerical values listed at the end of Sec. 6.4.3.

6.4.5 Evaluation of $D(0, s; \mathbf{k})$ in four dimensions

One of the diagrams of $D(0, s; \mathbf{k})$ at $d = 4$ is

$$\mathbf{k} \circledast = \frac{2K_4}{\pi} \int_1^s q dq \int_0^\pi [I(|\mathbf{q} + \mathbf{k}|) - I(q)] \sin^2 \theta d\theta, \quad (148)$$

where the wave vectors of solid and dotted lines are within $[0, 1]$ and $[1, s]$, respectively. Here

$$I(q) = \mathbf{q} \text{ (loop) } = \frac{2K_4}{\pi} \int_{q-1}^1 k dk \int_{\hat{\theta}(q,k)}^{\pi} \frac{\sin^2 \theta d\theta}{q^2 + 2kq \cos \theta + k^2} \quad \text{for } 1 < q < 2. \quad (149)$$

A problem here is that $I(q)$, apparently, has a singularity at $q = 1$. Considering the limit $\lim_{\Delta \rightarrow 0} \lim_{k \rightarrow 0}$, the contribution of the region $1 + \Delta < q < s$ (for $1 < s < 2$) can be evaluated by the small- k expansion, as in Sec. 6.4.3, whereas the contribution of the region $1 < q < 1 + \Delta$ has to be considered separately. It yields

$$\mathbf{k} \text{ (loop) } = k^2 \times \frac{K_4}{8} \int_1^s (3I'(q) + qI''(q)) dq + \mathcal{R}_1(k) \quad \text{at } k \rightarrow 0, \quad (150)$$

where $\mathcal{R}_1(k)$ is the contribution of $1 < q < 1 + \Delta$ region. It is important in our consideration if $\lim_{k \rightarrow 0} \mathcal{R}_1(k)/k^2 \neq 0$. In any case, $\mathcal{R}_1(k)$ is independent of s , since $I(q)$ is s -independent and also the borders of the region $1 < q < 1 + \Delta$ do not contain s . The ‘‘regular’’ contribution of the region $1 + \Delta < q < s$ can be represented by the given integral, since $I'(q)$ is continuous and finite at $q = 1$ and $I''(q)$ is at least integrable. Moreover, it can be shown that $I''_+(1) := \lim_{q \rightarrow 1} I''(q)$ (where ‘‘+’’ means tending to 1 from above, $q > 1$) has a finite value.

According to (149), for $1 < q < 2$, we have

$$I'(q) = \frac{K_4}{\pi} \left\{ - \int_{q-1}^1 \sqrt{1 - a^2(q, k)} b(q, k) dk - 4 \int_{q-1}^1 k dk \int_{\hat{\theta}(q,k)}^{\pi} \frac{(q + k \cos \theta) \sin^2 \theta d\theta}{(q^2 + 2kq \cos \theta + k^2)^2} \right\}, \quad (151)$$

$$\begin{aligned} I''(q) = \frac{K_4}{\pi} \left\{ - \frac{1}{2} \int_{q-1}^1 \frac{a(q, k) b^2(q, k)}{\sqrt{1 - a^2(q, k)}} \frac{dk}{k} + 2 \int_{q-1}^1 \sqrt{1 - a^2(q, k)} \left[\frac{1 - k^2}{q^3} + b(q, k) (q + k a(q, k)) \right] dk \right. \\ \left. - 4 \int_{q-1}^1 k dk \int_{\hat{\theta}(q,k)}^{\pi} \left(\frac{1}{(q^2 + 2kq \cos \theta + k^2)^2} - \frac{4(q + k \cos \theta)^2}{(q^2 + 2kq \cos \theta + k^2)^3} \right) \sin^2 \theta d\theta \right\}, \quad (152) \end{aligned}$$

where $a(q, k) = \frac{1 - q^2 - k^2}{2kq}$ and $b(q, k) = \left(1 + \frac{1 - k^2}{q^2}\right)$. The integrand function is always finite for $I'(q)$, but it diverges at $q = 1$ and $\theta \rightarrow \pi$ in the last integral of $I''(q)$. Therefore we have analysed the contribution of the region $\theta_0 < \theta < \pi$ and $k_0 < k < 1$ to this integral, denoted as $I''_{\text{sing}}(q)$, where θ_0 and k_0 are constants. These are chosen such that $\pi - \theta_0$ is small, but k_0 can be any positive constant smaller than 1 if $q \rightarrow 1$. Since the remaining contribution to $I''(q)$ is certainly finite at $q \rightarrow 1$, it is clear that $I''_+(1)$ is finite if $I''_{\text{sing}}(q)$ is bounded at $q \rightarrow 1$. We have

$$I''_{\text{sing}}(q) = \dot{I}''(q; k_0, 1, \theta_0), \quad (153)$$

where

$$\dot{I}''(q; k_1, k_2, \theta_0) = \frac{2K_4}{\pi} \int_{k_1}^{k_2} k dk \int_{\theta_0}^{\pi} \frac{\sin^2 \theta d\theta}{q^2 + 2kq \cos \theta + k^2}. \quad (154)$$

The integration in (154) can be at least partly performed changing the integration order. It yields

$$\begin{aligned} \dot{I}(q; k_1, k_2, \theta_0) &= \frac{2K_4}{\pi} \int_{\theta_0}^{\pi} \left[\frac{1}{2} \ln \left(\frac{(k_2 + q \cos \theta)^2 + q^2 \sin^2 \theta}{(k_1 + q \cos \theta)^2 + q^2 \sin^2 \theta} \right) \right. \\ &\quad \left. - \cot \theta \left(\arctan \left(\frac{k_2 + q \cos \theta}{q \sin \theta} \right) - \arctan \left(\frac{k_1 + q \cos \theta}{q \sin \theta} \right) \right) \right] \sin^2 \theta d\theta. \end{aligned} \quad (155)$$

From (155) we find

$$\begin{aligned} \dot{I}''(q; k_1, k_2, \theta_0) &= \frac{2K_4}{\pi} \int_{\theta_0}^{\pi} \left(\frac{k_2^2 - q^2 - 4k_2 \cos \theta (q + k_2 \cos \theta)}{(q^2 + 2k_2 q \cos \theta + k_2^2)^2} \right. \\ &\quad \left. - \frac{k_1^2 - q^2 - 4k_1 \cos \theta (q + k_1 \cos \theta)}{(q^2 + 2k_1 q \cos \theta + k_1^2)^2} \right) \sin^2 \theta d\theta. \end{aligned} \quad (156)$$

$I''_{\text{sing}}(q)$ is evaluated by setting here $k_1 = k_0$ and $k_2 = 1$. In this case, the second term gives constant contribution at $q \rightarrow 1$, whereas the contribution of the first term for small $\hat{\Delta} = q - 1$ and small $\delta_0 = \pi - \theta_0$ can be evaluated as

$$I''_{\text{sing}}(q) \simeq \frac{2K_4}{\pi} \int_0^{\delta_0} \frac{2(\hat{\Delta} + \delta^2)\delta^2 d\delta}{(\hat{\Delta}^2 + \delta^2)^2}. \quad (157)$$

The used here approximation for the integrand function has vanishing relative error at $\hat{\Delta} \rightarrow 0$ and $\delta = \pi - \theta \rightarrow 0$. Since the integrand function is positively defined, this approximation gives vanishing relative error for the integral at $\hat{\Delta} \rightarrow 0$ and $\delta \rightarrow 0$. Taking into account that

$$\int_0^{\theta_0} \frac{2\hat{\Delta}\delta^2 d\delta}{(\hat{\Delta}^2 + \delta^2)^2} = \arctan \left(\frac{\theta_0}{\hat{\Delta}} \right) - \frac{\theta_0 \hat{\Delta}}{\hat{\Delta}^2 + \theta_0^2}, \quad (158)$$

and considering the limit $\hat{\Delta} \rightarrow 0$, we can conclude that $I''_{+}(1)$ is, indeed, finite. Moreover, numerical analysis shows that $I''(q)$ is almost linear function of q for small and positive $q - 1$, indicating that $I'''_{+}(1)$ is also finite.

It can be shown that the contributions of the vicinities of singular points (like $\mathcal{R}_1(k)$) are important at least for some of the considered here diagrams. In particular, different estimates of $\left(\mathbf{k} \text{ with a slash and a circle around it} \right)^{as}$ for $s = 1 + ds$ are inconsistent with each other if these contributions are neglected. One of the possibilities is

$$\begin{aligned} \mathbf{k} \text{ with a slash and a circle around it} &= \frac{2K_4}{\pi} \int_1^{1+ds} q dq \int_0^{\pi} [\tilde{I}(|\mathbf{q} + \mathbf{k}|) - \tilde{I}(q)] \sin^2 \theta d\theta \\ &= k^2 \times \frac{K_4}{8} \int_1^{1+ds} (3\tilde{I}'(q) + q\tilde{I}''(q)) dq + \mathcal{R}_2(k, s) \quad \text{at } k \rightarrow 0, \end{aligned} \quad (159)$$

where

$$\tilde{I}(q) = \mathbf{q} \begin{array}{c} \text{---} \\ \text{---} \end{array} = \frac{2K_4}{\pi} \int_1^{1+ds} k dk \int_{\hat{\theta}(q,k)}^{\pi} \frac{\sin^2 \theta d\theta}{q^2 + 2kq \cos \theta + k^2} \quad \text{for } 1 < q < 1 + ds. \quad (160)$$

The term $\mathcal{R}_2(k, s)$ is the contribution of vicinities of singular points $q = 1$ and $q = 1 + ds$. Expressions for $\tilde{I}'(q)$ and $\tilde{I}''(q)$ are the same as those for $I'(q)$ and $I''(q)$ (Eqs. (151) and (152)) with the only difference that the integration limits for k now are from 1 to $1 + ds$.

Another interesting possibility is to use the symmetry of the diagram $\mathbf{k} \begin{array}{c} \text{---} \\ \text{---} \end{array}$ with respect to the dotted lines, i. e., $\mathbf{k} \begin{array}{c} \text{---} \\ \text{---} \end{array} = 2 \mathbf{k} \begin{array}{c} \text{---} \\ \text{---} \end{array}$, where “ \sim ” means the constraint that the wave vector of the upper dotted line is larger in magnitude than that of the lower dotted line. It yields

$$\begin{aligned} \mathbf{k} \begin{array}{c} \text{---} \\ \text{---} \end{array} &= \frac{4K_4}{\pi} \int_1^{1+ds} q dq \int_0^{\pi} [\bar{I}(|\mathbf{q} + \mathbf{k}|, q) - \bar{I}(q, q)] \sin^2 \theta d\theta \\ &= k^2 \times \lim_{\Delta \rightarrow 0} \left[\frac{K_4}{4} \int_1^{1+ds} \left(3 \frac{\partial \bar{I}(q, p)}{\partial q} \Big|_{p=q-\Delta} + q \frac{\partial^2 \bar{I}(q, p)}{\partial q^2} \Big|_{p=q-\Delta} \right) dq \right] + \mathcal{R}_2^*(k, s) \quad \text{at } k \rightarrow 0, \end{aligned} \quad (161)$$

where

$$\bar{I}(q, p) = \frac{2K_4}{\pi} \int_1^p k dk \int_{\hat{\theta}(q,k)}^{\pi} \frac{\sin^2 \theta d\theta}{q^2 + 2kq \cos \theta + k^2}. \quad (162)$$

The term $\mathcal{R}_2^*(k, s)$ is the contribution of the region $0 < q_1 - q_2 < \Delta$, where \mathbf{q}_1 is the wave vector of the upper dotted line and \mathbf{q}_2 – of the lower dotted line. Expressions for $\partial \bar{I}(q, p)/\partial q$ and $\partial^2 \bar{I}(q, p)/\partial q^2$ are the same as those for $I'(q)$ and $I''(q)$ (Eqs. (151) and (152)) with the only difference that the integration limits for k now are from 1 to p .

Using the same estimation techniques as for the diagram $\mathbf{k} \begin{array}{c} \text{---} \\ \text{---} \end{array}$, we find that

$$\mathbf{k} \begin{array}{c} \text{---} \\ \text{---} \end{array} = -k^2 \times \frac{K_4^2}{4} ds + \mathcal{R}_2(k, s) + o(ds) \quad \text{at } k \rightarrow 0, \quad (163)$$

$$\mathbf{k} \begin{array}{c} \text{---} \\ \text{---} \end{array} = \mathcal{R}_2^*(k, s) + o(ds), \quad (164)$$

where (163) follows from (159) and (160), whereas (164) – from (161) and (162). The contribution of order $\mathcal{O}(ds)$ in (163) comes from

$$k^2 \times \frac{K_4}{8} \int_1^{1+ds} q \dot{I}''(q; 1, 1 + ds, \theta_0) dq,$$

where $\dot{I}''(q; 1, 1 + ds, \theta_0)$ is the main contribution to $\tilde{I}''(q)$, given by (156), which surprisingly appears to be of order unity, i. e., $-2K_4 + \mathcal{O}(ds)$ for $1 < q < 1 + ds$. As regards $\partial^2 \bar{I}(q, p)/\partial q^2$, the contribution of similar origin is $\lim_{\Delta \rightarrow 0} \dot{I}''(q; 1, q - \Delta, \theta_0)$, which is not of order unity, since the main terms of (156) cancel in this case. It follows from (163) and (164) that at least one of the terms $\mathcal{R}_2(k, s)$ and $\mathcal{R}_2^*(k, s)$ is important at $k \rightarrow 0$. The reason why such a term can appear

to be important is that, for any given \mathbf{k} , the small- \mathbf{k} expansion might be convergent or valid only at large enough (k -dependent) distances from the singular point(s).

Further on, we will use (161)–(162), since one can prove the following statement for $\mathcal{R}_2^*(k, s)$:

Lemma. *If, in four dimensions, $\mathcal{R}_2^*(k, s)$ is proportional to k^2 at $k \rightarrow 0$ (with non-zero proportionality coefficient), then it is also proportional to $\ln s$, i. e., $\mathcal{R}_2^*(k, s) \propto k^2 \ln s$ at $k \rightarrow 0$.*

Proof. Recall that $\mathcal{R}_2^*(k, s)$, evaluated in the limit $\lim_{\Delta \rightarrow 0} \lim_{k \rightarrow 0}$, is given by $2 \mathbf{k} \begin{array}{c} \text{---} \\ \text{---} \end{array}$, where the wave vector $1 < q_1 < s$ corresponds to the upper dotted line and q_2 – to the lower dotted line with a constraint $0 < q_1 - q_2 < \Delta$. Let us denote by $\hat{\mathcal{R}}(k; \Delta, s_1, s_2, \Lambda_1, \Lambda_2)$ the term $2 \mathbf{k} \begin{array}{c} \text{---} \\ \text{---} \end{array}$ with $s_1 < q_1 < s_2$, $0 < q_1 - q_2 < \Delta$ and wave vectors within $[\Lambda_1, \Lambda_2]$ for the solid line. Then we have $\mathcal{R}_2^*(k, s) = \hat{\mathcal{R}}(k; \Delta, 1, s, 0, 1) = \hat{\mathcal{R}}(k; \Delta, 1, s, 0, 1/s) + \hat{\mathcal{R}}(k; \Delta, 1, s, 1/s, 1)$. The latter term can be well estimated by the small- \mathbf{k} expansion, used throughout here, first calculating the block $\mathbf{q} \begin{array}{c} \text{---} \\ \text{---} \end{array}$, which is an analytic function of q within $q \in [1/s, 1]$ for small Δ . Besides, it vanishes at $\Delta \rightarrow 0$. Therefore, we have $\hat{\mathcal{R}}(k; \Delta, 1, s, 1/s, 1) = A(\Delta) k^2$ at $k \rightarrow 0$, where $A(\Delta) \rightarrow 0$ at $\Delta \rightarrow 0$. Consequently, this term is negligible in the considered limit at the conditions of the *Lemma*. Rescaling in this case yields $\hat{\mathcal{R}}(k; \Delta, 1, s, 0, 1/s) = s^{-2} \hat{\mathcal{R}}(sk; s\Delta, s, s^2, 0, 1) = \hat{\mathcal{R}}(k; \Delta, s, s^2, 0, 1)$ at $k \rightarrow 0$. Here $s\Delta$ is replaced by Δ , since certain limit exists at $\Delta \rightarrow 0$ according to the conditions of the *Lemma*. Summarising these relations, we have

$$\mathcal{R}_2^*(k, s) = \hat{\mathcal{R}}(k; \Delta, 1, s, 0, 1) = \hat{\mathcal{R}}(k; \Delta, s, s^2, 0, 1) \quad (165)$$

in the limit $\lim_{\Delta \rightarrow 0} \lim_{k \rightarrow 0}$. We can also use the diagram identities

$$\hat{\mathcal{R}}(k; \Delta, 1, s, 0, 1) + \hat{\mathcal{R}}(k; \Delta, s, s^2, 0, 1) = \hat{\mathcal{R}}(k; \Delta, 1, s^2, 0, 1) = \mathcal{R}_2^*(k, s^2). \quad (166)$$

Combining (165) and (166), we obtain

$$\mathcal{R}_2^*(k, s^2) = 2 \mathcal{R}_2^*(k, s) \quad \text{for } s > 1 \quad (167)$$

and, consequently, $\mathcal{R}_2^*(k, s) \propto \ln s$. \square

Summarising the estimation of the diagrams of $D(0, s; \mathbf{k})$, we conclude that the necessary consistency condition (146) can be satisfied only if $\lim_{k \rightarrow 0} \mathcal{R}_1(k)/k^2 = 0$ holds, since $\mathcal{R}_1(k)$ is a quantity of order $(ds)^0$ (independent of ds). Furthermore, $\mathcal{R}_2^*(k, s) = Ck^2 \ln s$ must hold to satisfy this condition, where C is a constant. Here we allow also a possibility $C = 0$, referring to the case where $\lim_{k \rightarrow 0} \mathcal{R}_2^*(k)/k^2 = 0$. If the latter limit is non-zero, then (146) requires that $\mathcal{R}_2^*(k) \propto k^2$ at $k \rightarrow 0$ holds, i. e., the conditions of the *Lemma* are satisfied and, therefore, $\mathcal{R}_2^*(k, s) = Ck^2 \ln s$ holds with $C \neq 0$. Taking into account these facts and the discussed here estimations of the diagrams $\mathbf{k} \begin{array}{c} \text{---} \\ \text{---} \end{array}$ and $\mathbf{k} \begin{array}{c} \text{---} \\ \text{---} \end{array}$ (see Eqs. (150) and (161)), the condition (146) can be satisfied only if $D^{as}(0, s; \mathbf{k})$ has the form

$$\begin{aligned} D^{as}(0, s; \mathbf{k}) &= k^2 \times \frac{K_4}{8} \left\{ (3I'(1) + I''_+(1)) ds + \left(2I''_+(1) + \frac{1}{2} I'''_+(1) \right) (ds)^2 \right. \\ &\quad \left. + C_1 \ln(1 + ds) + C_2 (ds)^2 + \mathcal{O}((ds)^3) \right\}, \end{aligned} \quad (168)$$

where $C_1 = 8C/K_4$ and

$$C_2 = 2 \lim_{ds \rightarrow 0} \left\{ \frac{1}{(ds)^2} \lim_{\Delta \rightarrow 0} \int_1^{1+ds} \left(3 \frac{\partial \bar{I}(q, p)}{\partial q} \Big|_{p=q-\Delta} + q \frac{\partial^2 \bar{I}(q, p)}{\partial q^2} \Big|_{p=q-\Delta} \right) dq \right\}. \quad (169)$$

Moreover, it is necessary that the expansion coefficients at ds and $(ds)^2$ are consistent with those in (146).

Let us first consider a possibility that $\lim_{k \rightarrow 0} \mathcal{R}_2^*(k, s)/k^2 = 0$. In this case $C_1 = 0$ and (168) is inconsistent with (146) already at the $\mathcal{O}(ds)$ order according to the numerical estimates $I(1) \simeq 0.285932K_4$, $I'(1) \simeq -1.217996K_4$, $I''_+(1) \simeq 4.9873K_4$, $I'''_+(1) \simeq -22.02K_4$. In this case, only $I'(1)$ and $I''_+(1)$ are important. The above values satisfy certain relations

$$I(1) - J(1) = \frac{1}{2}K_4, \quad (170)$$

$$I'(1) - J'(1) = -K_4, \quad (171)$$

$$I''_+(1) - J''(1) = 5K_4, \quad (172)$$

$$I'''_+(1) - J'''(1) = -22K_4, \quad (173)$$

$$3I'(1) + I''_+(1) = \frac{4}{3}K_4 \quad (174)$$

within the given numerical accuracy, indicating that these values are not accidental. Moreover, we have verified that the values of the derivatives, calculated directly from (151) and (152), are consistent with the ones obtained by a numerical differentiation of $I(q)$ and $I'(q)$. Therefore, we are confident about these values.

According to (174), the coefficient at $k^2 ds$ in (168) is $K_4^2/6$ if $C_1 = 0$, whereas it must be $-K_4^2/12$ if (146) holds. The coefficient C_1 can be adjusted to reach the consistency at the $\mathcal{O}(ds)$ order. In this case we set $C_1 = -2K_4$, and evaluate C_2 to check the consistency at the $\mathcal{O}((ds)^2)$ order. It is based on the observation that

$$\lim_{\Delta \rightarrow 0} \left. \frac{\partial \bar{I}(q, p)}{\partial q} \right|_{p=q-\Delta} = B_1 (q-1) \quad \text{at } q-1 \rightarrow 0, \quad (175)$$

$$\lim_{\Delta \rightarrow 0} \left. \frac{\partial^2 \bar{I}(q, p)}{\partial q^2} \right|_{p=q-\Delta} = B_2 (q-1) \quad \text{at } q-1 \rightarrow 0 \quad (176)$$

hold with some constants B_1 and B_2 . Then we have

$$C_2 = 3B_1 + B_2. \quad (177)$$

Recall that $\partial \bar{I}(q, p)/\partial q$ and $\partial^2 \bar{I}(q, p)/\partial q^2$ are given by modified Eqs. (151) and (152), where the integration limits for k are set from 1 to p . The coefficient B_1 can be easily calculated analytically: $B_1 = -\left(\frac{\sqrt{3}}{\pi} + \frac{1}{3}\right)K_4$. For B_2 , we use the decomposition

$$B_2 = \tilde{B}_2 + \hat{B}_2, \quad (178)$$

where \tilde{B}_2 comes from the integrals over k , whereas \hat{B}_2 – from the double integral over k and θ . A simple calculation yields $\tilde{B}_2 = \frac{2K_4}{\sqrt{3}\pi}$. In the double integral for \hat{B}_2 , we have $\hat{\theta}(q, k) = 2\pi/3 + \mathcal{O}(ds)$, therefore this integration limit can be set $2\pi/3$ in the actual calculations up to the order of $(ds)^2$. Then we perform the integration over k to obtain the result in the form of (156), i. e.,

$$\begin{aligned} & \lim_{\Delta \rightarrow 0} \left[\frac{2K_4}{\pi} \int_{2\pi/3}^{\pi} \left(\frac{(q-\Delta)^2 - q^2 - 4(q-\Delta)\cos\theta(q + (q-\Delta)\cos\theta)}{(q^2 + 2(q-\Delta)q\cos\theta + (q-\Delta)^2)^2} \right. \right. \\ & \left. \left. - \frac{1 - q^2 - 4\cos\theta(q + \cos\theta)}{(q^2 + 2q\cos\theta + 1)^2} \right) \sin^2\theta d\theta \right] = \hat{B}_2 (q-1) \quad \text{at } q-1 \rightarrow 0. \quad (179) \end{aligned}$$

Based on the numerical analysis of (179), we have estimated $\hat{B}_2 \simeq 5.654K_4$. Note that

$$3B_1 + \hat{B}_2 = 3K_4 \quad (180)$$

holds within the numerical error, indicating that 5.654 is not an accidental value. Hence, $C_2 = \left(3 + \frac{2}{\sqrt{3}\pi}\right)K_4$ holds at least within the actual numerical accuracy. Summarising these estimates, the expansion coefficient at $(ds)^2$ in (168) within the given numerical accuracy is

$$\frac{K_4}{8} \left\{ 2I''_+(1) + \frac{1}{2}I'''_+(1) - \frac{1}{2}C_1 + C_2 \right\} = \frac{5}{12}K_4^2, \quad (181)$$

if $C_1 = -2K_4$. According to (146), the coefficient $1/24$ is expected instead of $5/12$ obtained here. Again, it is very unlikely that such a simple rational coefficient could be accidentally produced by an erroneous numerical calculation. It shows that the necessary consistency condition (146) and, consequently, also (129) is not satisfied. According to the consideration in Sec. 6.4.2, it implies that $D(0, \infty; \mathbf{k})/k^2$ diverges at $k \rightarrow 0$.

Recall that this result is obtained, assuming that finite (or zero) limits exist in (24), (61), (63) and (94). This is the best scenario for the ε -expansion, since divergent limits would imply the instability of the RG flow. Moreover, the universality of the critical exponent η , determined from the fixed-point equation $c' = c$ in Sec. 3.5, as well as the $\propto k^{-2+\eta}$ scaling of the fixed-point correlation function considered in Sec. 6.2, is ensured by the existence of these limits.


The derived here contradiction implies that, even in this best case, the perturbative ε -expansion-based renormalization of $X(\mathbf{k})$ on the critical surface is not fully consistent with the one produced by the exact rescaling (91) of the expected asymptotic expansion (103) at small k . Note that the renormalization considered in Sec. 6.3 is an infinite-scale ($m \rightarrow \infty$) renormalization at $\varepsilon \rightarrow 0$. If the ε -expansion works correctly there, then it turns out that an inconsistency appears on a finite renormalization scale considered in this section. This contradiction shows that the ε -expansion fails to give correct results in the actual test, despite of the fact that it is formally well defined and stable.

6.5 The two-point correlation function above the critical point

Consider now the inverse of the two-point correlation function above the critical point. It implies that $X(\mathbf{k})$ has to be positively defined for all \mathbf{k} when the diagrams are represented by \mathbf{k} -space integrals. As throughout the paper, we consider the domain $r = \mathcal{O}(\varepsilon)$ and $u = \mathcal{O}(\varepsilon)$, where the ε -expansion can be, in principle, valid. A problem here is such that the equation contains divergent diagrams. Namely, we have

$$\begin{aligned} X(\mathbf{k}) &= ck^2 - \frac{n+2}{2}u^2 \left\{ \mathbf{k} \text{ (diagram)} + \mathbf{k} \text{ (diagram)} + 3 \left(\mathbf{k} \text{ (diagram)} + \mathbf{k} \text{ (diagram)} \right) \right\} \\ &+ \left(r + \frac{n+2}{2}u \mathbf{0} \text{ (diagram)} \right) \left(1 - \frac{n+2}{2}u \mathbf{0} \text{ (diagram)} \right) + \mathcal{O}(\varepsilon^3) \end{aligned} \quad (182)$$

where the diagram $\mathbf{0} \text{ (diagram)}$ has to be calculated at $d = 4$ at this order of the ε -expansion. It diverges as $\propto \int_0^\Lambda k^{-1}dk$ within the ε -expansion. A standard idea, used in the perturbative renormalization, is to choose such values of the Hamilton parameters (coupling constants) at which the divergences cancel. It is also called renormalization. However, in this simple example, the cancellation (at $u \neq 0$) occurs if and only if $r + \frac{n+2}{2}u \mathbf{0} \text{ (diagram)} = 0$ holds. This is exactly

the condition of the critical surface (101). Hence, the cancellation never occurs slightly above the critical point, and such a renormalization method is not helpful here. Another question is whether a correct result is obtained, if the divergent diagram  is simply discarded. The answer is negative. Indeed, it can be easily checked that $X(\mathbf{k})$ obtained in this way is inconsistent with the exact rescaling relation (91). The latter finding is not surprising: in the diagrammatic perturbation theory this relation, similarly as the semigroup property and the s -independence of the fixed point of the RG transformation R_s , is a consequence of certain diagram rescaling and summation rules. These rules cannot work to give the expected result if some diagram is simply omitted.

In view of these facts, the applicability of such kind of perturbative renormalization, where coupling constants are adjusted to cancel the divergent terms or, alternatively, the divergent terms are simply discarded, is doubtful.

A serious idea is to perform the RG transformation until the model becomes sufficiently off-critical. It has been applied in the rigorous RG analysis in four dimensions [13, 19]. The only question, which might arise here, is how it can be done consistently within the ε -expansion in $4 - \varepsilon$ dimensions.

Certain method of calculation of the two-point correlation function has been considered in [12], which also resolves the problem of divergent diagrams. It, however, is not based on the ε -expansion, but on certain grouping of diagrams, in such a way that the true correlation function instead of the Gaussian one is related to the coupling lines. It naturally ensures the convergence of the diagrams of the reorganized perturbation theory and allows an analytic continuation of the obtained self consistent equations from the region $r > 0$ to the vicinity of the critical point.

7 Discussion

There are a lot of perturbative RG studies of the φ^4 model made in the past (see [2, 3, 4, 20] for a review). They can be classified as approximative treatments of the perturbation theory in view of our analysis, since a set of apparently irrelevant terms is neglected. Although a perturbative RG approach to critical phenomena never could be considered as a rigorous method, it is, nevertheless, possible to calculate exactly the perturbation terms and to take them into account in a systematic way. In particular, we find that there are many different terms to be included in the renormalized Hamiltonian up to the order of ε^3 , and these terms are relevant, as discussed at the end of Sec. 4. To the contrary, one usually finds that only few terms, i. e., those included already in the initial Hamiltonian (2) are relevant. A confusion about this might be caused by the fact that in the usual (non-rigorous) treatments one looks for the behaviour of individual terms and finds that most of them are shrinking in the renormalization procedure. It, however, is not a rigorous and even not a valid argument, since the $H^{(2m)}$ parts of (65) (as well as any part of $H^{(2m)}$ represented as a sum over diagrams of certain topology) result from many such individual terms, summing up to yield relevant contributions.

The results of perturbative calculations up to the order of ε^5 are reported in literature. These, however, are based on the Callan-Symanzik equation, but not on the Wilson's equation (3). The Callan-Symanzik equation, in fact, represents a scaling property for the Hamiltonian of the form (2). The approach, thus, relies on the assumption that all the relevant terms are included in the initial Hamiltonian, only the existing here coupling constants being renormalized. This assumption is not supported by our analysis: the perturbative renormalization based on first

principles (i. e., avoiding such assumptions via using (3)) produces additional relevant terms.

One believes that the ε -expansion, combined with the perturbative RG transformation, is able to describe correctly the small- \mathbf{k} asymptotic of the correlation functions and the related critical phenomena. The contradiction derived in Sec. 6.4 causes some doubts about it. Due to the formal character of the ε -expansion, one might happen that it describes the behaviour within any fixed range of non-zero wave vectors at $\varepsilon \rightarrow 0$ rather than the $k \rightarrow 0$ limit at a small, but fixed ε . Indeed, the contradiction might be caused by the fact that the non-Gaussian part of the Hamiltonian cannot be considered as a small perturbation, like in the ε -expansion, if one considers just the small- \mathbf{k} contribution responsible for the critical fluctuations, since the Fourier amplitudes of the relevant $\varphi_i(\mathbf{x})$ configurations diverge when $k \rightarrow 0$ at criticality.

8 Conclusions

1. A diagrammatic formulation of the perturbative renormalization has been provided (Sec. 2), which makes calculations of perturbation terms straightforward and transparent, avoiding any intermediate approximations.
2. The RG flow equations, including all terms up to the order of ε^2 , have been considered in Sec. 3. The tests of the expected properties, such as the semigroup property and the existence of an independent of the scale parameter s fixed point, have been performed. An expected scenario has been considered, where certain limits (Eqs. (24), (61) and (63)) exist. We have found that the tested here properties hold in this case.
3. An alternative approach has been briefly considered in Sec. 5, where ε is fixed and the coupling constant u is an expansion parameter. It has been shown that the fixed point is not s -independent in this case. The correctness of the known approach of the expansion at fixed dimension $d = 3$ has been questioned in this respect.
4. At the ε^3 order, the renormalized Hamiltonian contains several extra (φ^4 , φ^6 , φ^8) vertices, as compared to the bare Hamiltonian. All these terms are relevant, as discussed at the end of Sec. 4.
5. The two-point correlation function has been considered in Sec. 6 within the ε -expansion up to the order of ε^2 . It is consistent with the expected power-like behaviour at the fixed point (Sec. 6.2) if the limit (94) exists. Nevertheless, a contradiction with the exact rescaling of the small- \mathbf{k} asymptotic expansion on the critical surface has been found (Sec. 6.4).
6. Some aspects of the perturbative renormalization of the two-point correlation function slightly above the critical point have been briefly discussed in Sec. 6.5.

Concerning the points 4 and 5, several related issues have been discussed in Sec. 7.

References

- [1] K. G. Wilson, M. E. Fisher, Phys. Rev. Lett. **28**, 240 (1972)
- [2] Shang-Keng Ma, Modern Theory of Critical Phenomena, W.A. Benjamin, Inc., New York, 1976

- [3] J. Zinn–Justin, *Quantum Field Theory and Critical Phenomena*, Clarendon Press, Oxford, 1996
- [4] H. Kleinert, V. Schulte–Frohlinde, *Critical properties of ϕ^4 theories*, World Scientific (2001)
- [5] C. G. Callan, *Phys. Rev. D* **2**, 1541 (1970)
- [6] K. Symanzik, *Commun. math. Phys.* **18**, 227 (1970)
- [7] K. Symanzik, *Commun. math. Phys.* **23**, 49 (1971)
- [8] B. Delamotte, *Am. J. Phys.* **72**, 170 (2004)
- [9] D. Brydges, J. Dimock, T. R. Hurd, *Commun. Math. Phys.* **198**, 111 (1998).
- [10] T. Koma, H. Tasaki, *Phys. Rev. Lett.* **74**, 3916 (1995).
- [11] J. Kaupužs, *Int. J. Mod. Phys. C* **16**, 1121 (2005)
- [12] J. Kaupužs, *Ann. Phys. (Leipzig)* **10**, 299 (2001)
- [13] T. Hara, private communication
- [14] G. Parisi, *Cargèse Lectures 1973*, published in *J. Stat. Phys.* **23**, 49 (1980)
- [15] E. Brézin, J. C. Le Guillou, J. Zinn–Justin, in *Phase Transitions and Critical Phenomena*, edited by C. Domb, and M. S. Green (Academic, New York, 1976), Vol. 6.
- [16] J. C. LeGuillou, J. Zinn–Justin, *Phys. Rev. Lett.* **39**, 95 (1977)
- [17] G. A. Baker, B. G. Nickel, M. S. Green, D. I. Meiron, *Phys. Rev. Lett.*, **36**, 1351 (1976)
- [18] G. A. Baker, B. G. Nickel, D. I. Meiron, *Phys. Rev. B*, **17**, 1365 (1978)
- [19] T. Hara, H. Tasaki, *J. Stat. Phys.* **47**, 92 (1987).
- [20] A. Pelissetto, E. Vicari, *Physics Reports* **368**, 549 (2002)